land

MDPI

Article

A Method for Determining the Affected Areas of High-Alpine Mountain Trails

Andrej Bašelj [1,*], Damijana Kastelec [2], Mojca Golobič [1], Žiga Malek [1,3] and Žiga Kokalj [4]

[1] Department of Landscape Architecture, Biotechnical Faculty, University of Ljubljana, 1000 Ljubljana, Slovenia; mojca.golobic@bf.uni-lj.si (M.G.); ziga.malek@bf.uni-lj.si (Ž.M.)
[2] Department of Agronomy, Biotechnical Faculty, University of Ljubljana, 1000 Ljubljana, Slovenia; damijana.kastelec@bf.uni-lj.si
[3] Novel Data Ecosystems for Sustainability (NODES) Research Group, International Institute for Applied Systems Analysis (IIASA), 2361 Laxenburg, Austria
[4] Head of Remote Sensing Department, Institute of Anthropological and Spatial Studies, Research Centre of the Slovenian Academy of Sciences and Arts, 1000 Ljubljana, Slovenia; ziga.kokalj@zrc-sazu.si
* Correspondence: andrej.baselj@bf.uni-lj.si

Abstract

High-mountain areas with sensitive ecosystems are experiencing a steady increase in visitation, with visitors progressively moving outside designated trails, generating pressures on the natural environment. In extensive areas with numerous access points, it is difficult to monitor visitors' movement and resulting impacts. This article describes a method for combining various data sources and approaches to determine affected areas, including their locations and extent. The method combines (1) field-mapping, (2) remote-sensing data display analysis, and (3) processing of publicly available GNSS tracks from sports applications, using 46 test plots along a selected trail to Mount Triglav in Slovenia. Affected-area surfaces and their spatial overlap were compared across the three approaches. The usefulness of remote-sensing displays and GNSS tracks for determining and predicting affected areas was assessed by reference to field measurements. A linear regression model showed that the display-analysis approach can explain 52.7% of the variability in field-mapping approach, while GNSS tracks do not provide enough information nor the accuracy comparable to field surveys. This study can help other researchers and nature-protection managers in selecting most suitable data derived from non-traditional sources to improve delineation of hiking trails and estimation of potential pressures on fragile environments.

Keywords: mountain trails; off-trail movement; estimation of affected areas; GNSS movement tracks; remote sensing data; lidar; sports and recreation applications; fieldwork measurements

Academic Editor: Enrique Serrano Cañadas

Received: 3 December 2025
Revised: 16 January 2026
Accepted: 20 January 2026
Published: 22 January 2026

1. Introduction

With increasing visitation to high-mountain areas worldwide, including the Alpine region of Slovenia [1–5], pressures on protected areas and the natural and cultural values within their boundaries are likewise intensifying. High visitation levels not only intensify pressures on sensitive Alpine ecosystems [4,5] but also influence visitor safety [6] and diminish the experiential quality that pristine mountain environments are expected to provide [7–11].

Although comprehensive area management is essential to achieve compromises and the balance between the capacities of a given space and the visitors needs [12,13], the

network of designated hiking trails constitutes the component of public infrastructure with the most direct and decisive impact on visitors behaviour [14,15]. Systems of maintained and equipped trails (paved and marked paths, signposted and equipped with safety installations) [14,16,17], provide visitors with safe access to their destinations, support diverse recreational activities, enable wildlife and plant observation, and offer opportunities to learn about natural and cultural attractions [18]. Designated trails, therefore, play a central role in shaping visitor behaviour, spatial movement, and overall experience [16,19].

When the maintenance of the trail network is insufficient or does not meet the needs and demands, visitors, for various reasons, begin to move spontaneously and diffusely across the terrain, outside designated trail surfaces. This behaviour results in the formation of affected areas, which are informal, non-designated trails that are generally narrower and up to twice as steep as official paths [16]. As a result, they are more susceptible to erosion, soil loss, muddiness, and lateral widening [15,20]. Repeated off-trail movement further accentuates these impacts: habitat patches become fragmented [17]; sensitive Alpine vegetation suffers trampling damage and recovers slowly [4,5]; plant community composition becomes less diverse [5]; and invasive species may spread more readily [4,16,21]. Wildlife habitats are similarly affected, as movement outside designated trails can alter their abundance, species representation, or behaviour patterns [16–18]. As animals can adapt to crowded trails, the stress caused by spontaneous and scattered individual movement outside trails and peak visiting times is considerably greater [22].

Spontaneous, informal paths respectively affected areas are the most common consequence (impact) of recreational use of space [23,24], often generating conflicts between visitor interests and conservation objectives [25]. Predicting and monitoring their impacts is particularly challenging in extensive areas with open access through numerous uncontrolled entry points [3,26], or in remote regions where neither visitor monitoring nor field-based condition assessments are systematically ensured, or where such efforts are financially prohibitive for site managers.

In such contexts, advances in Global Navigation Satellite System (GNSS) technologies, Geographic Information Systems (GIS) [22], increasingly affordable GNSS devices [27], and the rapid growth of publicly available spatial data from online platforms have proven highly effective for monitoring recreational use [28]. Numerous studies have combined these technologies with direct (field measurements) and indirect (computer processing and analysis) analytical methods to address a wide range of issues related to the occurrence of affected areas. These include the quantification of patches due to habitat fragmentation [16], the identification of popular routes and areas with notably high densities of affected areas [16,28,29], the assessment of how visitor numbers influence the affected areas formation where official paths are absent [22], the measurement of impacts on trail erosion, wildlife disturbance and vegetation degradation [4,5,18,30,31], analyses of the physical structure, usage, and the function of hiking trails [12]; and evaluations of usage intensity and the expansion of informal paths [22], etc.

The use of user-generated spatial content, including GNSS transmitters and mobile device data (as GNSS movement tracks), georeferenced photographs, and social media posts, has shown a strong correspondence with field-based observations. Freely accessible spatial data have proven practical, widely available, and cost-effective [26]. These data can effectively supplement existing monitoring techniques and provide meaningful insights into both visitor numbers and their spatial behaviour impacts [28,32].

Existing research has primarily focused on documenting the various impacts, consequences, and issues that affected areas pose for individual components of the natural environment (wildlife, vegetation, geomorphology, etc.) [31]. Studies have mapped the spatial distribution and density of affected surfaces and tested the advantages of combining

different methods, techniques, and heterogeneous data sources [28,32,33]. How to examine the detailed, precise location of affected areas adjacent to official, designated trails, however, remains unknown, as studies measuring the actual spatial extent, such as the surface area (in m^2) of affected areas resulting from visitors moving outside the designated trails area, are lacking.

A new perspective on affected areas is proposed, viewing them as a potential indicator of the cumulative effects on the environment and landscape. In this sense, they reflect impacts on vegetation, wildlife, and abiotic components, as well as on the visual image and experiential quality of the landscape. In the proposed method, multiple data sources—namely, aerial orthophotos, airborne laser-scanning (ALS) data, and freely available GNSS movement tracks from sports applications—were combined with field measurements and computer-based analysis to identify the locations of affected areas and estimate their actual spatial extent (surface area in m^2). We applied this method along a selected mountain trail in Triglav National Park, where we quantified the extent of affected areas across 46 test plots and compared the values obtained by using different methodological approaches.

The high-mountain Alpine area of Triglav National Park is among the oldest protected areas in Europe, with the first proposal for its protection dating back to 1906. Covering 840 km^2, it is also the largest protected area in Slovenia, characterised by a high degree of natural ecosystem preservation and a network of 826 km of maintained mountain trails. It receives approximately two million visitors annually [2,34]. Affected areas, such as bypasses, shortcuts, side paths, parallel tracks, hunting trails, and other informal paths, are a common occurrence throughout the park.

Park managers monitor visitation in selected areas and along mountain trails using on-site counters, with many sites experiencing heavy use, particularly during peak season [35]. They also report the frequent posting of digital GNSS movement tracks outside designated trail areas on various sports applications, which is problematic in high-mountain environments both from a visitor-safety perspective and due to the potential for conflict, as such GNSS movement tracks (and the corresponding informal paths) often cross private land [35,36]. The relevance of this issue is further demonstrated by the establishment of quiet zones, introduced to mitigate the disturbance of wildlife caused by human activities [2,34,36].

Three key questions were addressed: firstly, the determination of the location of affected areas; secondly, the quantification of the extent of affected areas along the selected mountain trail to Triglav (expressed in m^2 across 46 test plots) as identified by each methodological approach—and thus by each data source; and thirdly, the assessment of the degree of spatial correspondence (intersection) between the affected areas delineated using the different approaches. By comparing these results, the accuracy with which remote-sensing data displays and user-generated GNSS movement tracks describe and predict the affected areas identified through field mapping was assessed.

2. Materials and Methods—Development of the Method for Determining Affected Areas

Affected areas along the selected mountain trail were determined across 46 test plots using three different approaches: (1) field measurement and mapping (hereafter: field surveys), (2) delineation of affected areas based on the processing and overlay of remote-sensing data displays (hereafter: displays), and (3) processing of user-generated GNSS movement tracks obtained from sports and recreation applications (hereafter: GNSS tracks).

The long-term state of affected areas, as represented by field surveys, displays, and GNSS tracks collected over a multiple-year period (2009–2024), was compared. In addition,

the state of affected areas derived from GNSS tracks for more recent and shorter time intervals (June–September, 2021–2024, and separately for 2024) was also compared.

The affected areas were determined by following the sequence of steps outlined in Scheme 1. For the mountain-trail area, all publicly available spatial datasets were obtained from publicly accessible sources. This was followed by a field survey, during which we mapped the trail route, measured its width, and identified and photo-interpreted the affected areas along the trail. Test plots were then established along the selected mountain trail, forming the analytical framework for determining affected areas. Next, several consecutive field surveys were conducted, during which we mapped the centrelines of the affected areas within each test plot. Computer-based analyses and remote-sensing data processing were subsequently utilised to refine the mapped trail route and calculate its surface area, which was then subtracted from the test plots. Through visual interpretation of remote-sensing displays, the centrelines and polygons of affected areas on the test plots were delineated. This was followed by the acquisition and processing of publicly available GNSS user-movement tracks from nine online sports and recreation applications. Next, estimated widths were assigned to the centrelines and GNSS tracks, surface areas were calculated, and the affected areas for all three methodological approaches (field surveys, remote-sensing data displays, and GNSS tracks) were determined by applying the same procedure. Finally, GIS was used to calculate spatial overlap on the test plots and intersections among the approaches, and the resulting values were compared using statistical analysis.

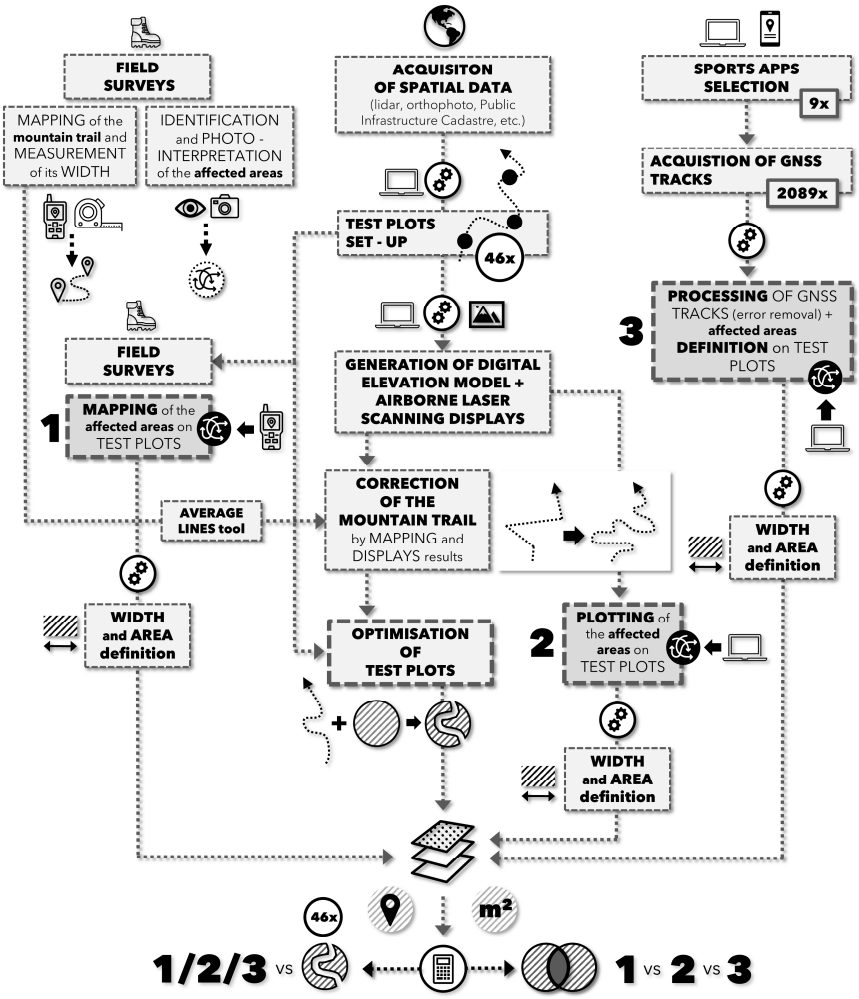

Scheme 1. Workflow for Determining Affected Areas.

2.1. Study Area, Selected Mountain Trail and Set-Up of Test Plots

For the study area, we selected the mountain trail leading from Rudno Polje (1347 m a.s.l.) to Triglav (2864 m a.s.l.) through Kredarica (2515 m a.s.l.), and returning from Triglav to Rudno Polje via Planika (Figure 1). This is one of the longest and most scenic mountain routes to the summit of Triglav (15.8 km), which includes sections of all three difficulty categories—easy, difficult, and very difficult. The trail traverses both open terrain (11.78 km) and forested areas (4.02 km), and crosses a variety of surface types, including forest, meadows and pastures, scree slopes, gravel-covered slopes, and entirely rocky terrain. This ensures a sufficiently diverse testing environment. Although the entire Triglav massif experiences high seasonal visit [2], the selected mountain trail is among the most popular and heavily used routes due to its high elevation (1347 m a.s.l.) [37] well-maintained, and internationally recognised trailhead at Rudno Polje, which features a large parking area, a tourist and recreation centre, and an international biathlon venue [36].

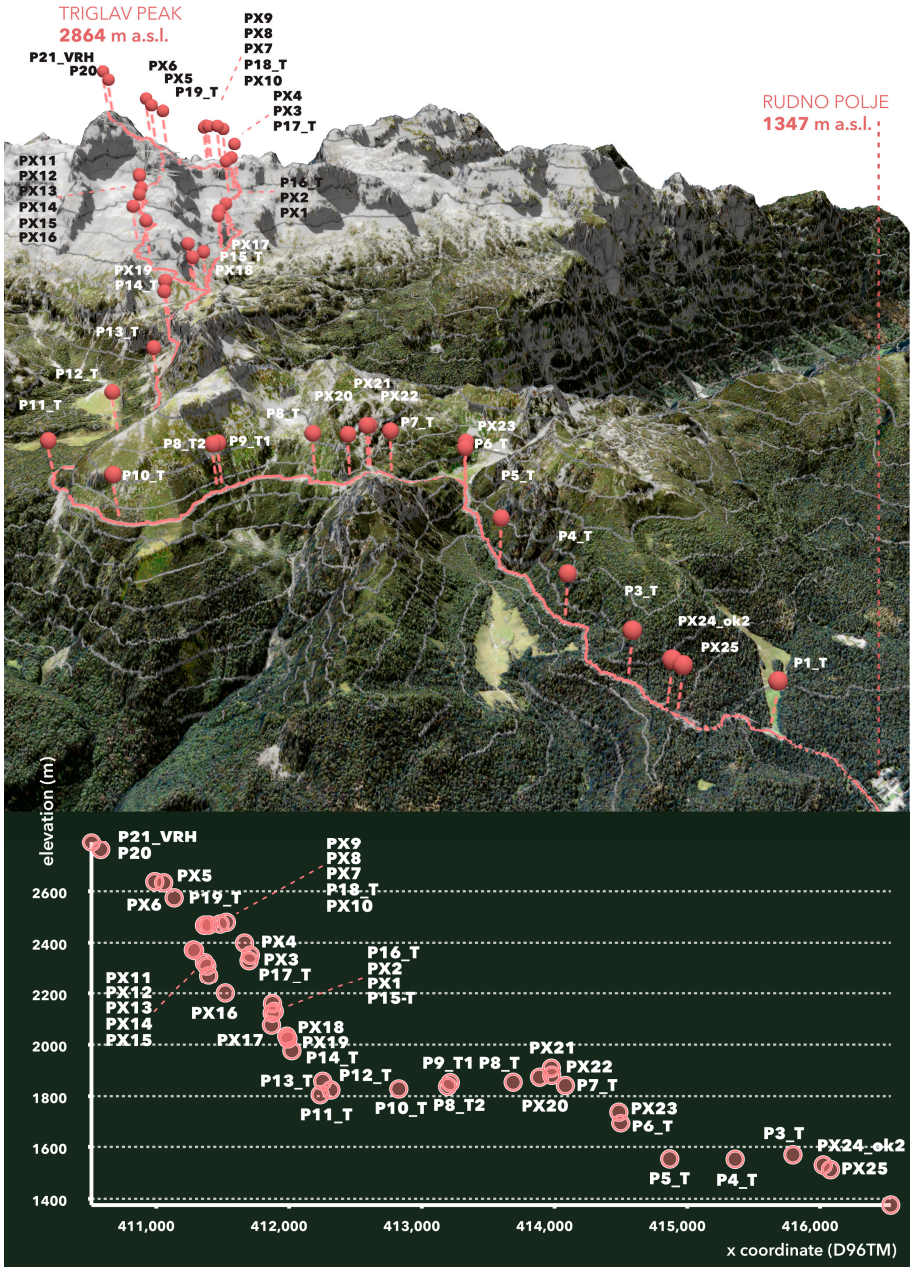

Figure 1. Selected mountain trail to Triglav with the locations and altitudes of the test plots.

Along the Triglav mountain trail, 21 test plots were initially established at regular intervals of 700 m. In doing so, all trail difficulty categories and all relevant surface and cover types were included (Table S1, Supplementary Materials). Based on a visual analysis of the actual condition of the affected areas in the field, an additional 27 test plots were subsequently identified. Two plots were later excluded due to a change in the official route alignment, where a newly marked section followed a former affected area (a shortcut). A total of 46 test plots were included in the study.

Each test plot is circular with a radius of 7.5 m, corresponding to an area of 176.7 m^2—or 175.8 m^2 when calculated using a geodetic buffer instead of the planar method, as the former is more suitable for local-scale distance calculations in a projected coordinate system [38,39]. Field mapping of affected areas in challenging and exposed terrain was conducted using a Garmin GPSMAP 66sr handheld GNSS device (Garmin Ltd., Olathe, KS, USA), which allows users to assign a radius to each point and provides an audible alert when the radius is reached.

The radius length was determined empirically during the initial field survey, where we found that most affected areas were located within this distance. Given the extremely rugged terrain, including trails cut into steep slopes and narrow ridge sections, this represented a reasonable maximum radius for the test plots.

After correcting the trail route through field surveys and display approaches, and by measuring its width, we created a polygon layer representing the trail surface, which was then clipped from test plot areas, as shown in Figure 2. All areas within each test plot but outside the trail surface polygon were therefore considered potentially affected areas. The trail surface area within individual test plots ranged from 7.9 m^2 (4.5%) to 65.1 m^2 (37.0%), with half of the test plots containing less than 17.2 m^2 (9.8%) of trail surface.

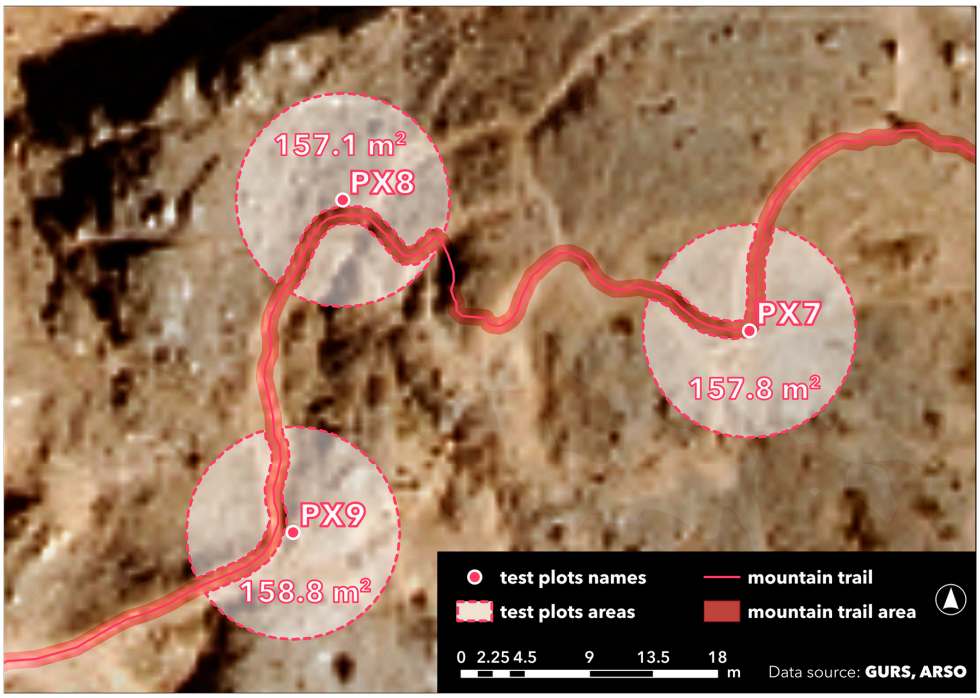

Figure 2. Test plots with delineated mountain trail surface. Light-shaded paths represent affected areas.

2.2. Field Surveys—Mapping the Mountain Trail and Affected Areas

Fieldwork was conducted over five survey campaigns (13–15 July, 15 August, 21–23 September 2022, and 17–18 July, 20 August 2023), corresponding to the period when mountain huts were open. The precise trail alignment was recorded using three

devices by repeatedly walking the route along the officially marked trail. Additionally, we mapped the centrelines of affected areas outside the designated trail area.

We used a Garmin GPSMAP 66sr handheld GNSS device, one of the most advanced handheld receivers available, capable of recording positions at one-second intervals and with a tested horizontal positional accuracy of 1.83 m [40]. In addition, we used a Suunto 9 Baro smartwatch (Suunto Oy, Vantaa, Finland) and a OnePlus 8T smartphone (OnePlus Technology Co., Ltd., Shenzhen, China), which is capable of multi-frequency GNSS reception. Location data were recorded using ten different applications: Garmin Connect for the handheld device, Suunto app for the smartwatch, and AllTrails, Fatmap, Gaia, Komoot, Relive, Sports Tracker, Strava, and Wikiloc for the smartphone [41–50]. These devices were intentionally chosen over professional surveying instruments to realistically imitate the equipment typically used by visitors to the mountain trail.

GNSS tracks collected during fieldwork were used to correct the official trail alignment [51], which was too generalised for the purposes of determining affected areas. Accurate trail geometry is essential for reliably identifying affected areas adjacent to the trail, as previous studies have emphasised the importance of precise and detailed trail-network data for distinguishing on-trail from off-trail movement [32]. The vector trail data obtained from official records [51] were therefore refined using the same approaches and datasets that were applied to delineate the affected areas.

For this purpose, a combination of aerial orthophotos, airborne laser-scanning (ALS) displays (see Section 2.3), and field-recorded GNSS tracks was used. A total of 88 GNSS tracks were recorded as point clouds (16 Garmin Connect, 21 Suunto App, and 51 from other applications) and subsequently converted into polylines. Because these lines do not coincide perfectly—owing to differences in device accuracy, application behaviour, current weather conditions, signal interference, and the number of available satellites—their geometries required harmonisation. To address this, Esri (Redlands, CA, USA) developed the Average Lines tool [52] at our request. The tool adjusts a reference line by calculating the mean or median position of all lines used within a specified search distance. Several averaged trail lines were generated, and those with the highest positional reliability were selected as reference lines. These included the tracks recorded using the handheld GNSS device, the smartwatch, and the smartphone running the Strava application, which logs activity at one-second intervals.

The averaged trail lines were used to determine the actual alignment of the marked mountain trail, particularly in sections of smooth rocky walls where movement requires technical equipment (iron rungs, fixed cables, and pegs), and in heavily eroded areas where the presence of numerous parallel paths makes it impossible to identify the main trail (Figure 3). In such cases, the combination of orthophotos and ALS displays does not provide sufficiently reliable information on the trail alignment.

The total length of the corrected mountain trail is 15,798.5 m, which is 932 m longer than the original official record. The updated trail alignment was submitted to the Alpine Association of Slovenia, which, as the custodian of the national mountain-trail cadastre, incorporated it into the official records and forwarded it to the Surveying and Mapping Authority of the Republic of Slovenia.

The trail width was measured at 58 points using a measuring tape. Its average width is 1.4 m. In the lower section, where the trail passes forest, it is wider and measures up to 4.5 m, while in the upper section, along an exposed rocky ridge, it narrows to 0.6 m (as illustrated by the examples in Figure 4). Within the 46 test plots, we identified affected areas and recorded the centrelines of these areas using GNSS devices (86 lines in total). All test plots were also photographically documented.

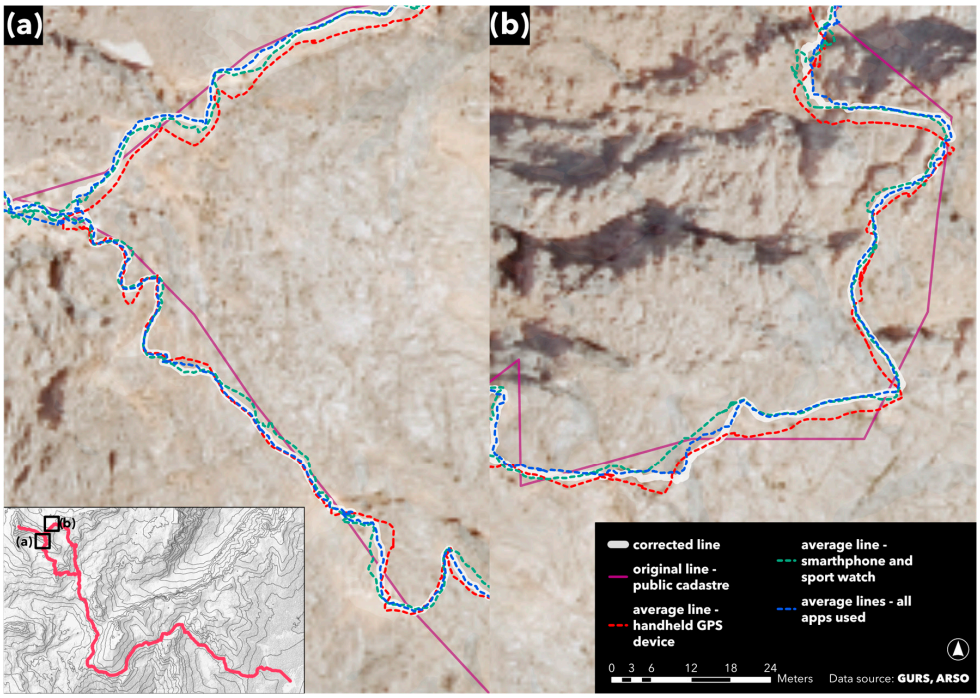

Figure 3. Illustration of the correction of the mountain trail route above the mountain huts: (**a**) rocky section uphill from the Planika; (**b**) rocky section uphill from the Kredarica.

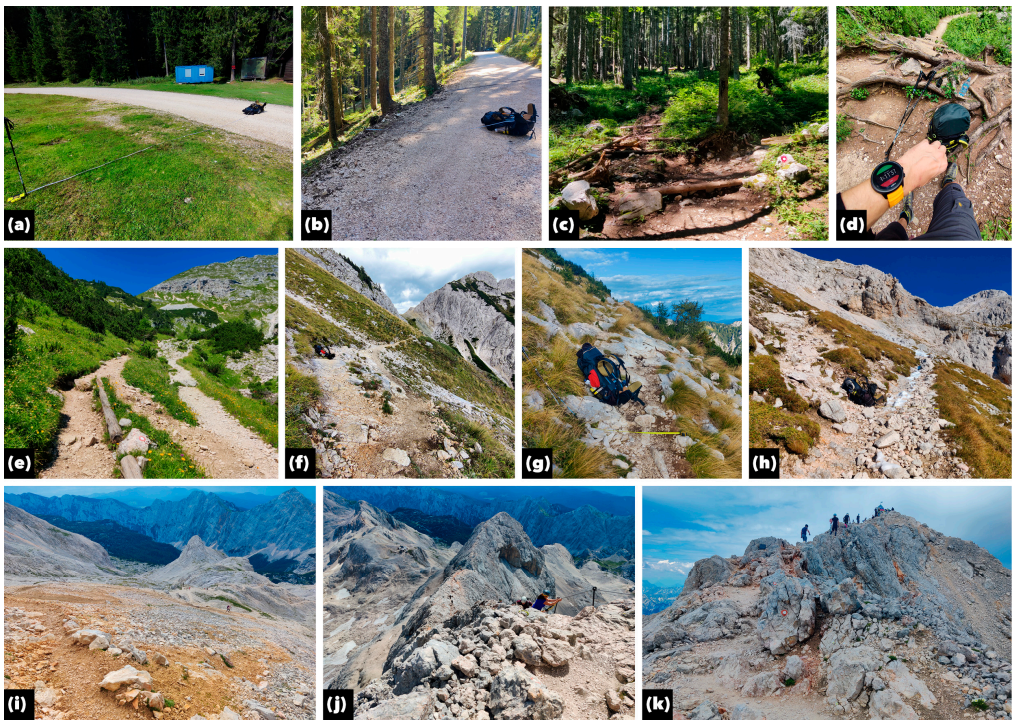

Figure 4. Mapping of affected areas during the field surveys was conducted within the test plots representing different substrate categories (Table S1, Supplementary Materials). Examples of substrate types along the trail from the trailhead toward the summit include: (**a**,**b**) compacted sand and soil with grass cover; (**c**,**d**) soil with a humus layer, sandy debris, individual stones, forest undergrowth, and roots; (**e**–**g**) sand, scree, scattered rocks, soil with grass cover, low vegetation, and shrubs; (**h**,**i**) sand, eroded soil, rocky debris, boulders, and patches of grass; (**j**,**k**) scree, stones, rocks, gravel, and eroded soil.

2.3. Delineation of Affected Areas on an Aerial Orthophoto and Airborne Laser Scanning Visualisations

For the area of the selected mountain trail, we obtained publicly available orthophotos with a spatial resolution of 0.5 m [53] as well as airborne laser-scanning (ALS, LiDAR) point clouds [54]. The point clouds were rasterized, the displays were calculated, and, using photo interpretation, the affected areas on the test plots were delineated.

The ALS Slovenia dataset used in this study was acquired in 2014–2015, with a nominal point density of only two pulses per m^2 in high-mountain areas [55]. The actual density is somewhat higher, but this is due to an error resulting from unintentionally duplicated points that were displaced by several centimetres [56]. Rasterisation was performed using a combination of Inverse Distance Weighted (IDW) and Natural Neighbour interpolation to generate a digital elevation model with a spatial resolution of 0.5 m. This combination of these two methods is particularly suitable for representing fine, small-scale local variations in the terrain [57,58], especially when interpolating irregularly spaced, sparse, or strongly linear point distributions [58] in forested mountain environments [59]. All raster and vector data processing was performed using ArcGIS Pro (version 3.5.4).

During rasterisation, we included points from the classes Never Classified (0), Ground (2), and Buildings (6). While the Ground class is essential, the Never Classified and Buildings classes may also contain potentially relevant details on micro-features such as dry-stone walls, trail-support structures, artificial stone cairns, boulders, and similar elements [60], which are important for accurately delineating both the alignment of the selected mountain trail and the affected areas adjacent to it. This is particularly relevant in locations where affected areas may be poorly visible due to substrate type or surrounding structures (e.g., bare rock surfaces without discernible soil, scree slopes with limited fine debris and larger stones).

Using raster-based functions from the Relief Visualisation Toolbox for ArcGIS Pro (version 3.5.4). [61,62], which enable the calculation of multi-layered and detailed terrain visualisations, we generated Prismatic Openness General, Sky-View Factor, and a customised visualisation based on the Principal Components Analysis of hillshading, where multiple visualisation layers were combined (Figure 5). The selected visualisations are particularly suitable for the effective identification of fine-scale geomorphological features [63,64].

Prismatic Openness General was computed using default settings, whereas the Sky-View Factor and the customised visualisation were produced using adjusted parameters. The Sky-View Factor was calculated with: number of search directions = 32, search radius = 5, and noise-removal level = 2 (medium). The customised visualisation combined: PCA as the base (value 0–2), Slope Gradient (default settings), Positive Openness (default settings), and Sky-View Factor (number of search directions = 16, search radius = 5, noise-removal level = 2, medium).

The ALS-derived visualisations were combined with the aerial orthophoto using different transparency levels and layer-blending modes (aerial orthophoto blending settings: Colour Dodge 50%, Lighten 70%, Multiply 0%, Darken 0%, Overlay 23%, Hard Light 35%, Colour 0%).

The varying colours of adjacent pixels in the aerial orthophoto, particularly in areas with heterogeneous land cover (e.g., mixtures of bare soil, rocky and grassy sections, and low to medium-height vegetation), produced strong contrasts. These provided a clear and plastic representation of terrain conditions, enabling a reliable differentiation between the selected mountain trail and the adjacent affected areas.

By combining aerial orthophoto with the ALS visualisations, we were able to reliably delineate both the mountain trail and the affected areas even in sections situated beneath high vegetation, in areas without soil or fine debris, and in many locations where complex

alpine terrain (e.g., cliffs, boulders, rock faces) cast shadows, but do not affect ALS-derived products. By systematically comparing the visualisation layers—alternating their visibility, toggling individual layers on and off, and adjusting display parameters such as histogram stretch, brightness curve, and contrast, we identified and delineated 88 lines representing traces of affected areas across the 46 test plots.

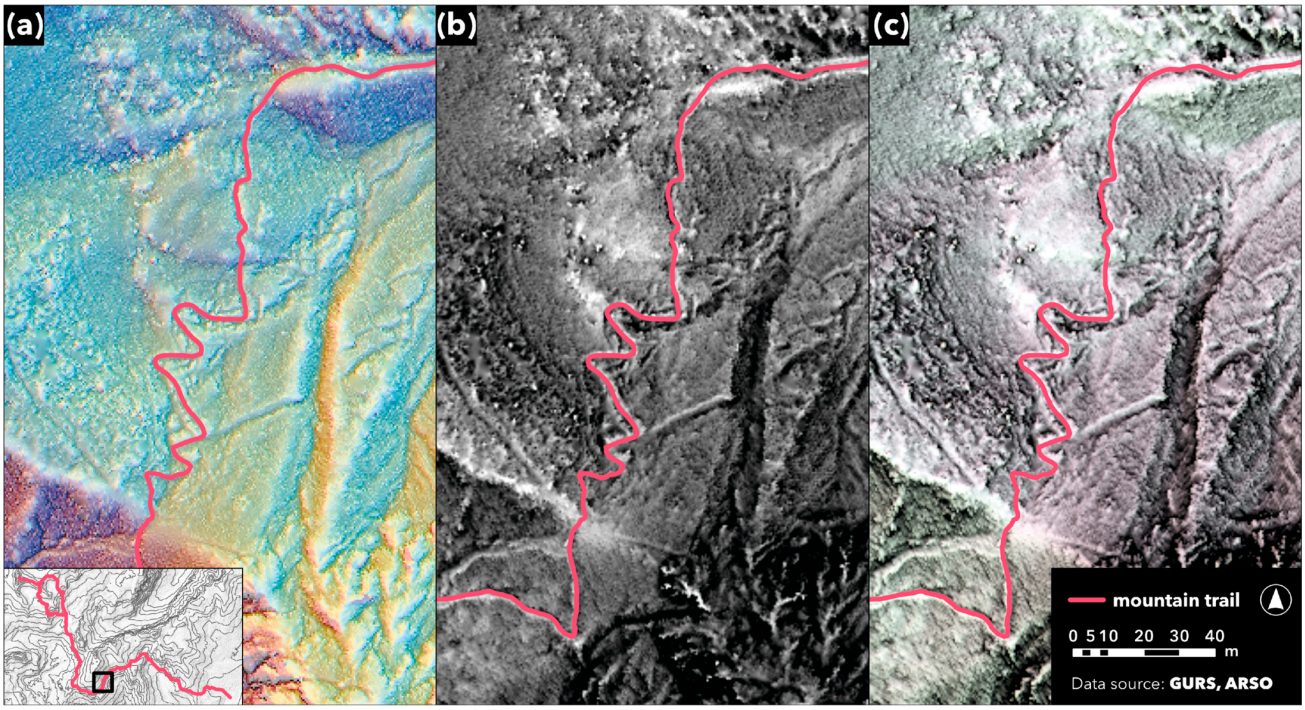

Figure 5. Using visual interpretation of Prismatic openness general (**a**), sky-view factor (**b**) and customised display (**c**) with a spatial resolution of 0.5 m, we determined the affected areas along the mountain trail.

2.4. Delineation of Affected Areas with Public Gnss Tracks from Sports Applications

Studies examining users' movement patterns in outdoor environments have highlighted numerous advantages of using GNSS tracks [28,32]. At the same time, they have highlighted uncertainties and potential biases that arise when data are collected in situations where participants are aware that their movements are being monitored.

Following the approach of Norman and Pickering [28], we manually retrieved user-movement data—GNSS tracks in GPX format—directly from online sports and recreation applications. Over several years of monitoring various hiking websites and forums [65–75], we initially identified 13 popular hiking applications to be assessed: AllTrails, Gaia GPS, Garmin Connect, Hiking Project, MapMyFitness, Outdooractive, Strava, Suunto Movescount, Wikiloc, Fatmap, Komoot, Relive, and SportsTracker [41,43–50,76–79].

The last four were excluded from further analysis because they do not allow GNSS track export or only offer this functionality in a paid version. As we aimed to obtain exclusively publicly accessible data, the following criteria were applied when evaluating the applications:

- The application's free version allows the upload, public sharing, and download of publicly posted GNSS tracks in GPX format;
- The downloaded user GNSS tracks are publicly posted and freely accessible;
- GNSS tracks are available for the study area.

The transfer of GNSS tracks (GPX files) was intentionally performed manually rather than using faster automated methods (e.g., scripted bulk downloading), as some on-

line applications prohibit automated data scraping and protect against it through Turing tests (CAPTCHA), which distinguish real users from computer-based systems (hardware or software).

GNSS tracks in GPX format were therefore downloaded through the user interfaces of the selected applications, which are largely similar in structure. Applications typically feature an integrated map that displays user activities at specific locations as icons. A dropdown menu on the left side of the map generally provides further information about each activity. As icon-based visualisation becomes ineffective when many activities overlap within the same area, some applications cluster GNSS tracks (e.g., AllTrails) [43], while others display them as simplified lines that reveal more detail when clicked (e.g., Gaia GPS) [45].

Among the various data points available for each recorded activity, the date of the activity was the key attribute for our analysis. All of the applications included in the study provide this information, except for Garmin Connect. For the latter, activity dates were determined manually through detailed inspection of individual GNSS tracks using the GPX Studio web application [80]. GNSS tracks were manually downloaded from the applications, regardless of the timing of the activity, based on a visual assessment of tracks from the trailhead to the summit. This approach proved more suitable than name-based searches (e.g., "Triglav," "Mali Triglav," "Rudno polje," "Pokljuka"), which tend to over-filter and constrain the results. We downloaded GNSS tracks for activity types typically performed on mountain trails on foot (e.g., running, hiking, walking, wildlife or plant observation).

In total, we manually downloaded 2089 GNSS tracks covering the period from 9 August 2009, to 17 November 2024 (Table 1), following procedures that ensured complete user anonymity. Only one track was available for 2009, while the highest number was recorded in 2024 (521 tracks). August accounted for the largest share of tracks overall (33%), while the highest number recorded on a single day was 14 (30 July 2024). The temporal distribution of the downloaded GNSS tracks by year and month (Figure 6) reflects the increasing popularity of sports applications, with a pronounced rise in 2017 (226%). From 2017 onwards, the peak summer months—June, July, August, and September—are consistently dominant, together representing 84% of all tracks. The influence of the COVID-19 pandemic is also evident, particularly the nationwide restrictions introduced in March 2020, which limited movement within municipal boundaries and temporarily halted outdoor recreational activities in Slovenia.

Table 1. Temporal range and number of user GNSS tracks by application.

Application Used	Number of GNSS Tracks Downloaded	Temporal Range of Downloaded GNSS Tracks
Wikiloc	744	4 January 2010–29 September 2024
All Trails	406	9 August 2009–7 November 2024
Suunto Movescount	295	21 November 2011–21 August 2021
Garmin Connect	288	7 April 2012–28 October 2024
Outdooractive	184	8 July 2010–28 October 2024
Strava	117	11 July 2016–17 November 2024
Gaia GPS	42	6 August 2015–15 November 2024
Map My Fitness	12	13 September 2013–15 July 2021
Hiking project	1	12 November 2022

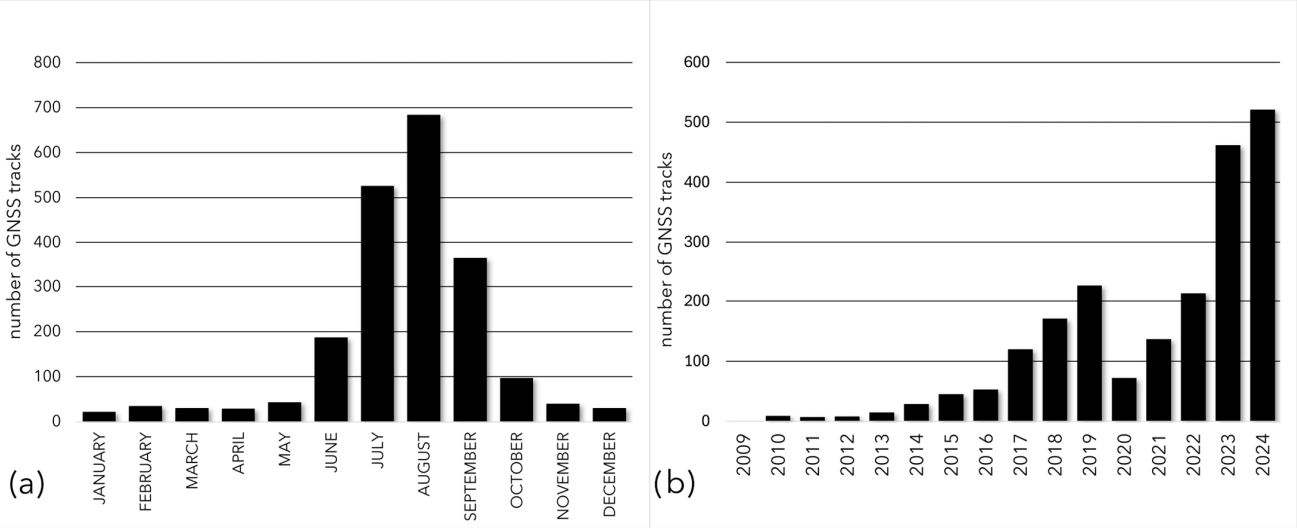

Figure 6. Number of GNSS tracks from nine sports applications by month (**a**) and by year (**b**).

After downloading the files, we converted them into the Esri file geodatabase format, projected them to the EPSG 3794 coordinate system (Slovenia 1996/Slovene National Grid), and connected the individual points into polylines. We used polylines instead of points to avoid the effects of point clustering, which occurs when users remain stationary while recording activity [32]. Files containing errors, empty files, and files comprising only a few unconnected points were excluded from further analysis. Consequently, 1999 GNSS tracks were retained for subsequent processing (Figure 7).

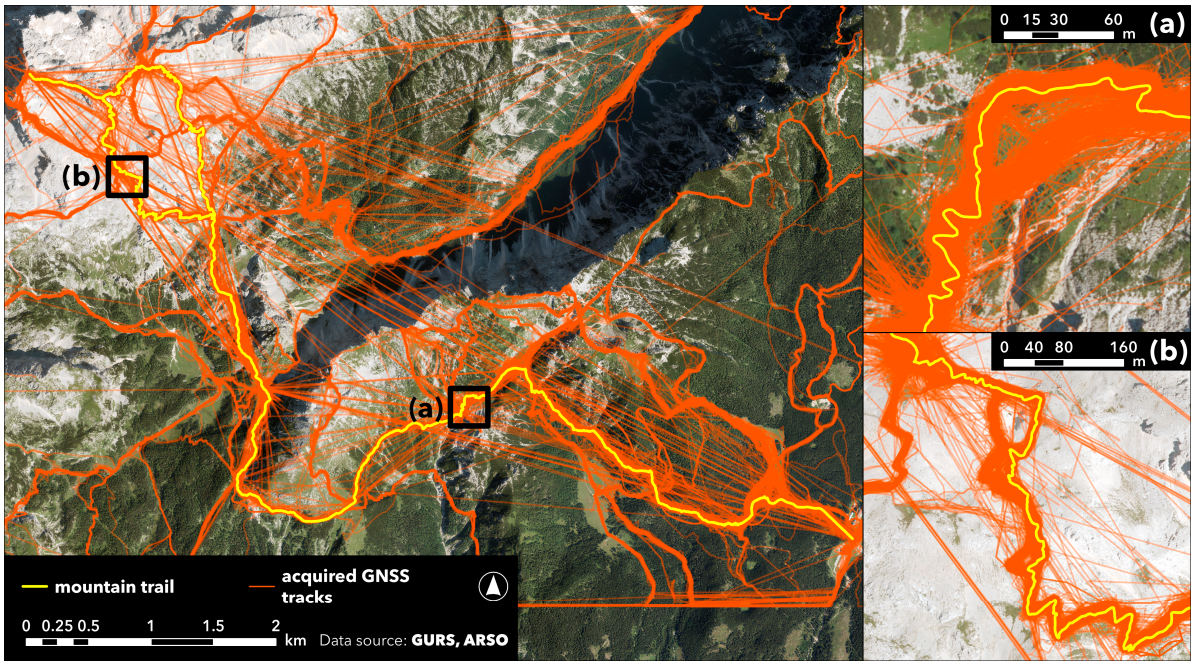

Figure 7. The GNSS tracks obtained for the selected mountain trail area exhibit substantial variability in positional accuracy: (**a**) a trail section on a slope with a mixture of sand, scree, soil with grass cover, low vegetation, and shrubs; (**b**) a trail section in a sandy and gravelly area near the Planika hut.

2.5. A Common Denominator—Integrating the Approaches for Determining Affected Areas

Using the three approaches described in previous sections, we obtained the centrelines of the affected areas (Scheme 2). Since our aim was to identify the affected areas rather than just their axes, we first converted the lines into surface polygons and then developed

a method for their meaningful comparison. The centrelines of affected areas were clipped to the extent of the 46 test plots. Next, we removed the area of the corrected mountain trail from each test plot, ensuring that only the lines of off-trail affected areas remained for further analysis. In total, we retained 86 lines mapped with field surveys, 88 lines delineated from displays, and 1772 GNSS track lines obtained from sports applications for further analysis.

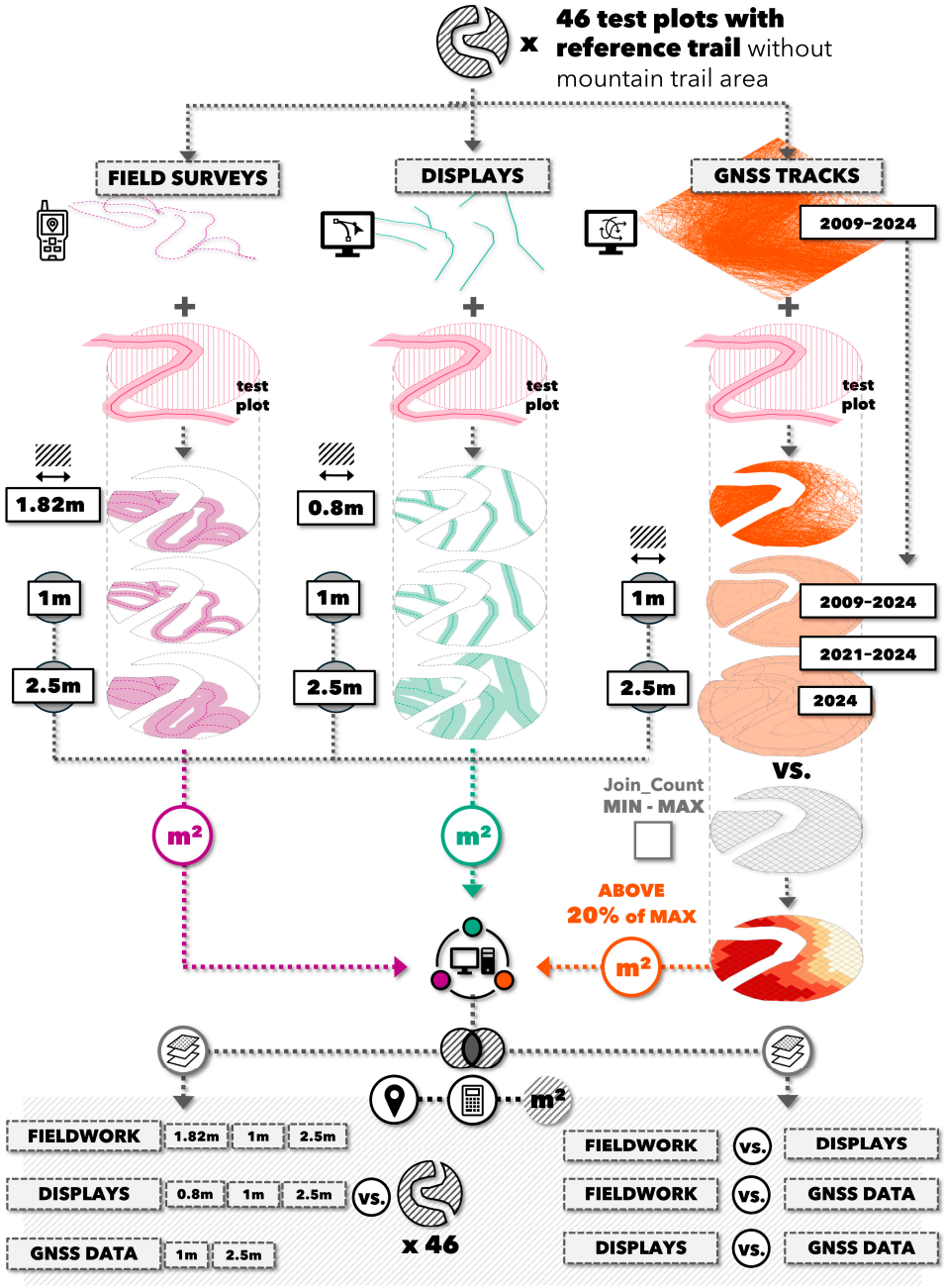

Scheme 2. Integration of approaches for determining affected areas.

To generate surface polygons of the affected areas, we considered the positional accuracy and spatial resolution of the devices and datasets used. In the field surveys, the centrelines of affected areas were mapped using a handheld navigation device with a verified horizontal positional accuracy of 1.82 m [40]. When identifying and delineating the centrelines of affected areas from displays, we worked with datasets having a spatial resolution of 0.5 m and determined that the average width of the affected areas was 0.8 m.

For the GNSS tracks, positional accuracy could not be established, as the applications do not provide information on the recording device (e.g., smartphone, sports watch, GPS receiver) or on the accuracy of the acquisition. Based on previous research on advances in positional accuracy and the performance of mobile and sports devices for location tracking [81–86], a positional accuracy value of 2.5 m was therefore applied to the GNSS tracks.

The identified widths were applied to buffer the centrelines of the affected areas, thereby generating surface polygons for each approach. For the field survey data, we applied a width of 1.82 m, for the displays a width of 0.8 m, and for the GNSS tracks a width of 2.5 m. The resulting surfaces within each test plot represent the potential affected areas for each respective approach.

In contrast to related studies, which assigned the positional accuracy width of the data (e.g., GNSS tracks) to the trail infrastructure—i.e., to the width of the analysed trail network ([32]: 8.99 m; [29]: 25 m; [28]: 30 m), these accuracy-related widths were attributed directly to the data themselves.

Since the aim was to assess how the use of different widths influences the calculated surface areas of affected zones and their spatial overlap, uniform widths were also applied to all affected-area centrelines, regardless of the approach. A width of 1 m, which is the standard applied by Slovenian trail markers when constructing new mountain trails [87], was used, along with a width of 2.5 m, the value determined for the GNSS tracks. The buffered surfaces derived from all centrelines were then merged by approach and by assigned width, clipped to the extent of the test plots, and subsequently used to calculate the affected-area surface for each of the 46 test plots.

As the surfaces derived from the GNSS tracks using the procedure described above do not reflect long-term, repeated off-trail movement (as each GNSS track represents only a single activity) and therefore do not represent the actual affected areas on the site, we considered only those surfaces where off-trail movement occurred multiple times.

To achieve this, we created a 0.5 m^2 square grid across each test plot (Figure 8). The choice of cell shape and size corresponds to the spatial resolution of the remote-sensing datasets used. Using a spatial join, we counted the number of individual affected-area surfaces that intersected each grid cell.

Because our aim was to retain only those grid cells indicating recurrent off-trail movement, all cells with values below 20% of the highest observed cell-coverage value across all test plots were excluded. The maximum value was 614, meaning that only cells intersected by at least 124 affected-area surfaces were included in the analysis. The threshold value was determined visually by examining the variability of the excluded surfaces and was subsequently verified using a statistical test (Section 3).

When analysing the frequency of GNSS tracks for the period 2009–2024, we identified a strong upward trend, which we attribute to the development and growing popularity of sports applications. We therefore sought to determine the influence of the temporal component, specifically, what does it mean to use GNSS tracks from shorter time periods, in which substantially fewer tracks are available. The aim was to assess the representativeness of GNSS tracks from more recent time periods and to determine the minimum temporal span required for GNSS data to reliably capture affected areas that reflect long-term conditions. In addition to the full 2009–2024 period, we therefore included GNSS tracks from selected shorter periods:

- The summer months of 2021–2024, when the highest numbers of GNSS tracks were recorded (June, July, August, September), and
- The 2024 summer season (June, July, August, September).

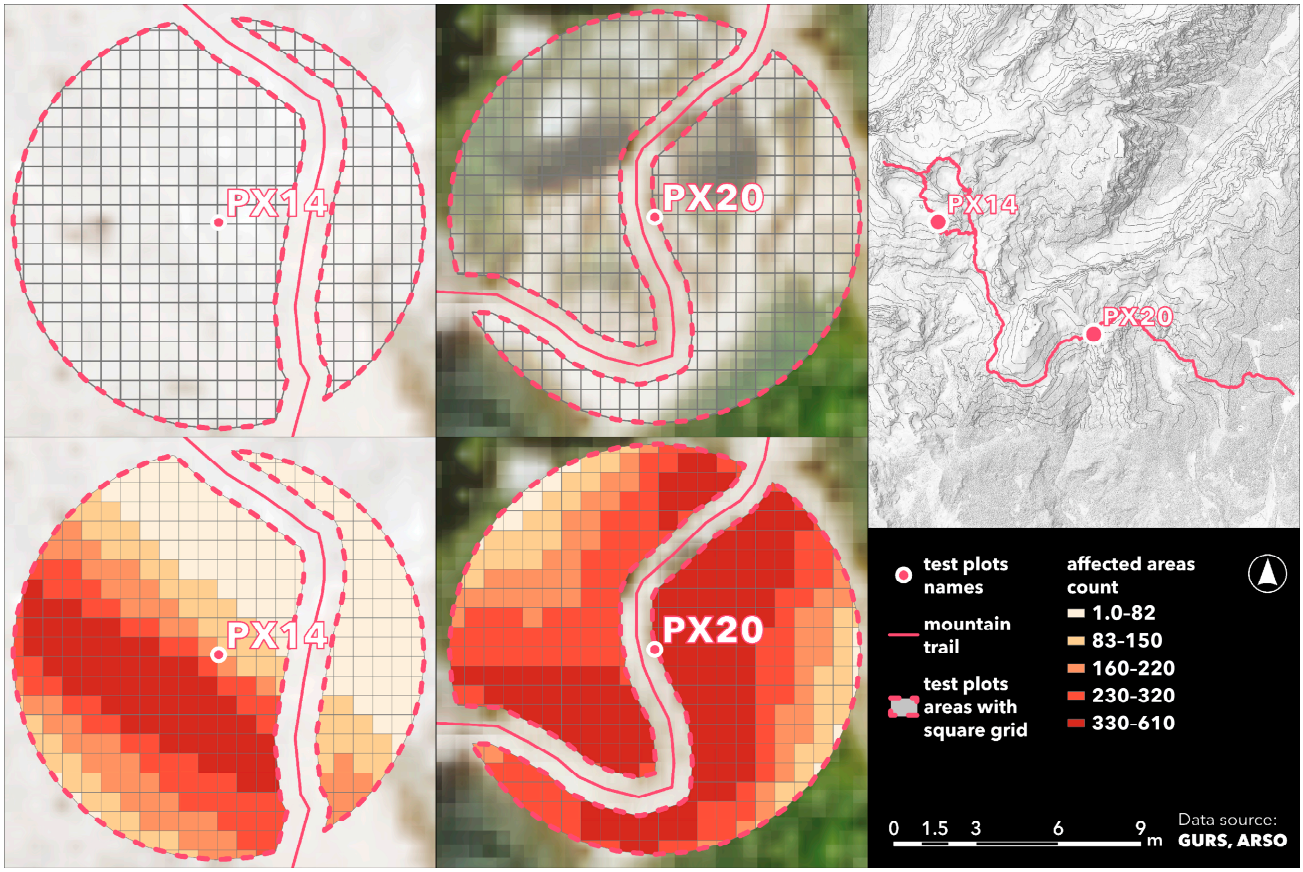

Figure 8. Examples of the results of spatial join of affected areas derived from GNSS tracks with a grid of squares on two different test plots.

For all three approaches, the selected widths, and the temporal periods of the GNSS tracks, we calculated the locations and extent to which the resulting surfaces overlapped each test plot. This was followed by an assessment of the pairwise spatial overlap between datasets to determine the extent to which the affected areas coincide. All data were compiled into a unified table and comparisons were performed. Descriptive statistics, including quantiles, means, standard deviations, and Pearson's correlation coefficients, were calculated to present the results. The linear regression model was used to explain the relationship between affected areas identified by the field survey approach and the other two approaches, with certain geographic variables (elevation, slope) and soil and vegetation variables (substrate, canopy cover) included as covariables.

3. Results

Affected areas were identified on 39 test plots through field surveys (examples with the largest and the smallest affected area are shown in Figure 9), on 31 plots through the analysis of displays, and on 45 plots by processing GNSS tracks (out of a total of 46 plots). All three approaches simultaneously identified affected areas on 30 of the 46 test plots (65%). Field surveys and display analysis simultaneously identified affected areas on 31 plots (67%), displays and GNSS tracks on 30 plots (65%), and field surveys and GNSS tracks on 38 plots (83%).

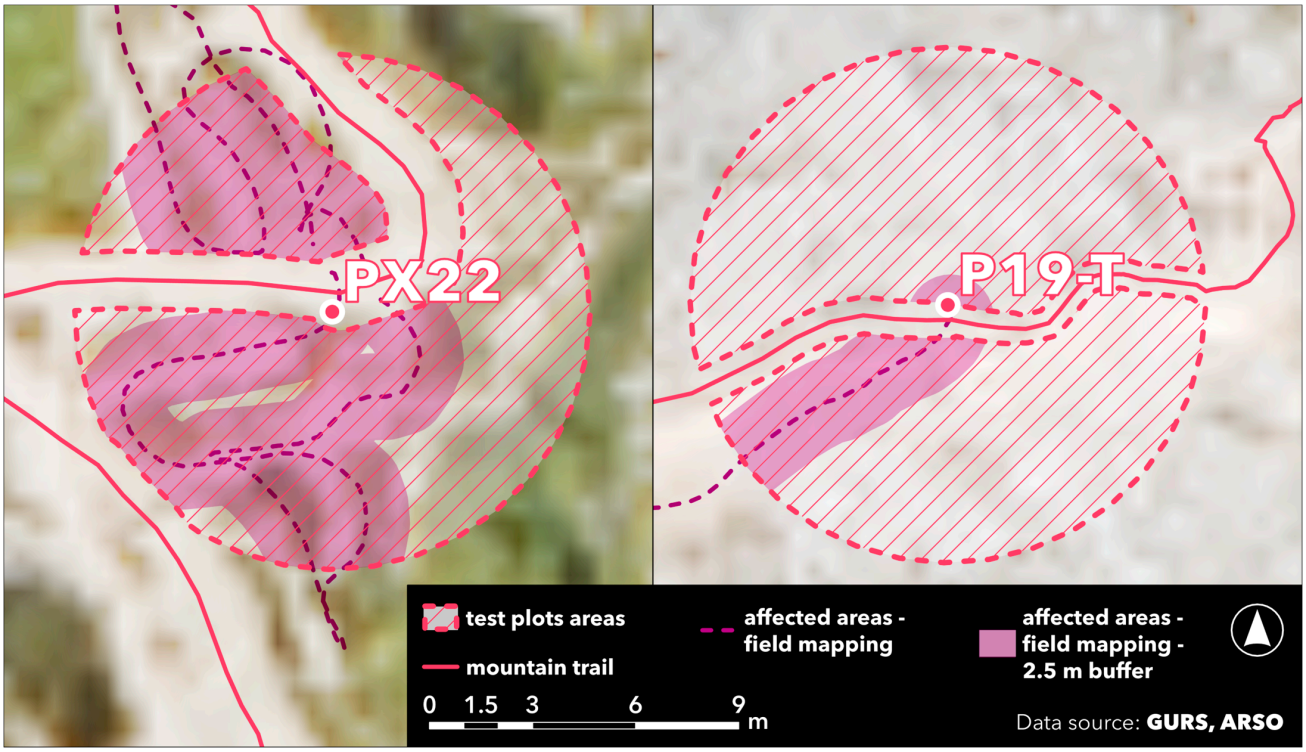

Figure 9. Test plot with the largest (**left**: PX22; 93.4 m^2) and the smallest (**right**: P19-T; 17.9 m^2) affected area as mapped in the field. We did not identify affected areas with field surveys on 7 test plots.

Field surveys confirmed the presence of affected areas on 100% of the plots where affected areas had been identified using the display analysis. However, the visual interpretation of the displays failed to detect affected areas on eight test plots. Consequently, the number of affected plots was underestimated by 20% (8 out of 39).

Field inspections also showed that GNSS tracks overestimate the extent of affected areas, as they indicated their presence on almost all test plots (45 compared to 39 identified in the field).

First, we compared the distribution of the percentage of affected areas across the 46 test plots, as determined by each approach, by the different widths used to generate the surfaces, and by the different temporal periods (the latter applying only to the GNSS tracks) (Figure 10).

The distribution of the estimated relative affected area, shown in Figure 10 by the boxplots (displaying the minimum and maximum values, the first and third quartiles, and the median), reveals that for the data obtained through the display analysis approach, and across all applied widths, at least one quarter of the test plots exhibited no affected areas (the minimum and first-quartile values are both zero). For the data derived using the other two approaches, at least one test plot likewise showed no affected areas.

As the applied width increases, the estimated extent of affected areas also increases. Consequently, the largest affected areas—regardless of the approach—are obtained when using the widest buffer, i.e., 2.5 m.

Increasing buffer width, however, did not contribute to higher correlations between the three approaches, as the input datasets differ substantially in both positional accuracy and data density. Due to abundance of GNSS tracks, the resulting affected areas fully covered test plot areas regardless of the selected buffer width.

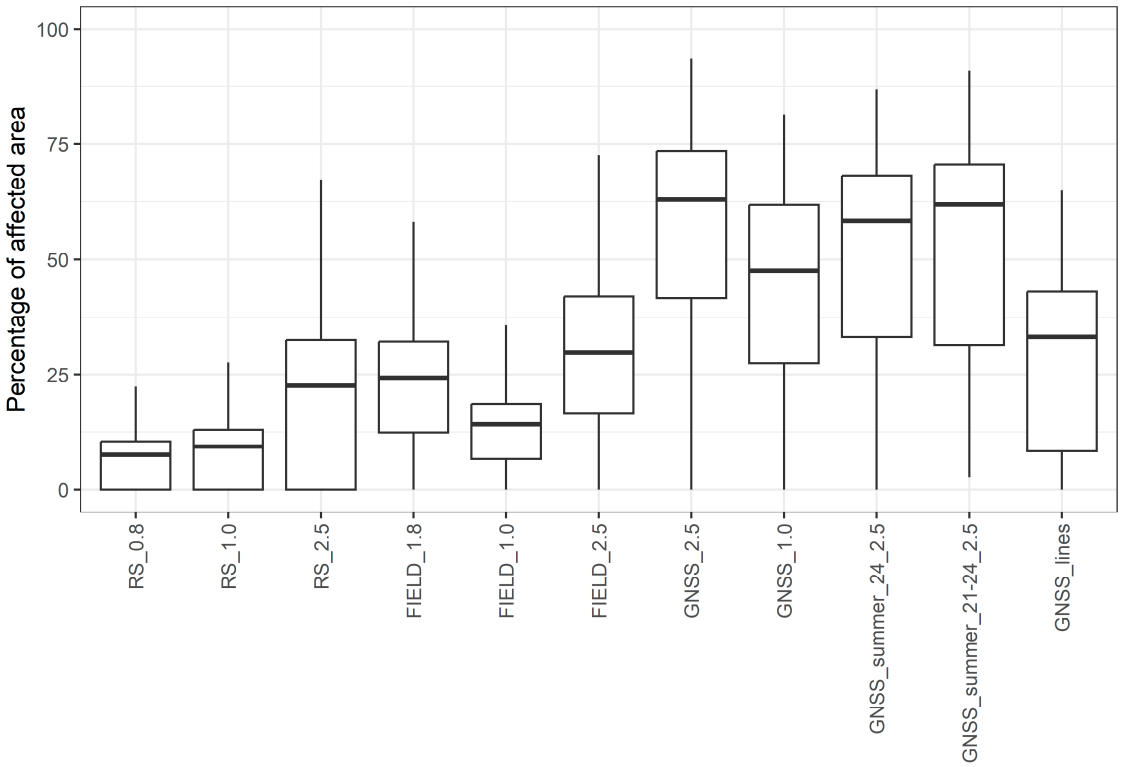

Figure 10. Boxplots of affected areas across the 46 test plots, with the area of the mountain trail removed, shown by the approach used to determine the affected areas, the widths applied to generate surface polygons, and the temporal period (for GNSS tracks). In this and all subsequent figures and tables, the following abbreviations are used: APPROACHES: FIELD SURVEYS—abbreviation "FIELD", REMOTE SENSING DATA VISUALISATIONS—abbreviation "RS", GNSS DATA—abbreviation "GNSS"; WIDTHS USED: buffer 0.8 m—abbreviation "0.8", buffer 1 m—abbreviation "1.0", buffer 1.82 m—abbreviation "1.8", buffer 2.5 m—abbreviation "2.5"; TEMPORAL PERIODS for GNSS tracks: 2009–2024—no abbreviation, summer months 2021–2024—abbreviation "summer_21_24", summer months 2024—abbreviation "summer_24".

For the GNSS tracks covering the entire period (2009–2024), we also tested an approach in which positional accuracy was not considered (GNSS_lines), using only direct overlap of GNSS tracks with the square grid on each test plot. Applying the same 20% threshold, we found that the resulting estimates of affected areas were smaller and more comparable to those obtained through the reference field surveys.

The results also show that the percentage of test-plot coverage by affected areas derived from GNSS tracks using the uniform 2.5 m width are very similar across the different temporal periods—and thus across the differing numbers of available GNSS tracks (2009–2024: 1772 tracks; 2021–2024 (June–September): 1068 tracks; and 2024 (June–September): 471 tracks) (Table 2).

Figure 11 shows that Pearson's correlation coefficient, as a measure of linear relationship. We used this coefficient as it is a widely used and easy to understand measure to study the relationship between two variables. The Pearson correlation coefficients indicate that the percentages of affected areas obtained through the display-analysis approach and the field survey approach are correlated (r = 0.7). In contrast, the percentage of affected areas derived from the GNSS-track analysis approach shows no correlation with either the display-based estimates or the field survey estimates.

Table 2. Descriptive statistics for the percentage of affected area determined using three different approaches, with three widths for the field surveys and displays, and two widths for the GNSS tracks. For the latter, at a width of 2.5 m, three different temporal periods were analysed. The minimum value is 0% for all cases. S_e denotes the standard error.

Approach	Min (%)	Max (%)	Median (%)	Mean (%)	S_e (%)
FIELD_1.8	0.00%	58.16%	24.29%	22.92%	2.23%
FIELD_1.0	0.00%	35.74%	14.15%	13.44%	1.37%
FIELD_2.5	0.00%	72.65%	29.82%	29.72%	2.78%
RS_0.8	0.00%	22.20%	7.47%	7.19%	0.93%
RS_1.0	0.00%	27.61%	9.29%	8.95%	1.16%
RS_2.5	0.00%	67.32%	22.48%	21.82%	2.76%
GNSS_2.5	0.00%	93.43%	62.98%	55.26%	3.64%
GNSS_1.0	0.00%	81.48%	47.58%	42.84%	3.39%
GNSS_summer_21_24_2.5	2.62%	90.84%	61.97%	52.75%	3.71%
GNSS_summer_24_2.5	0.00%	86.87%	58.42%	49.92%	3.64%
GNSS_lines	0.00%	64.95%	33.21%	29.34%	2.90%

Figure 11. Scatterplot matrix showing the relationships between the estimates of affected areas obtained using different approaches. Pearson correlation coefficients are shown above the diagonal.

The percentage of affected areas determined from the GNSS tracks is high because the large number of tracks produced surfaces that, regardless of the applied width, almost entirely covered the test-plot areas. As noted before, varying the widths within a given

approach proved unnecessary, and the percentages of affected areas obtained from GNSS tracks across different temporal periods were also strongly related.

For the GNSS-based approach, this means that recent GNSS data collected over a single season (e.g., June–September 2024), when sports applications are already well established and widely used—and when the number of available tracks is the highest—are fully comparable to the results derived from much longer temporal spans (e.g., 2009–2024), when such sports applications were less common or still in development.

We also examined the suitability of the threshold used to determine when a GNSS tracks-derived surface should be considered as affected area. To do this, we calculated the affected areas using several different thresholds (10%, 15%, 20%, 25%, 30%, 35%, 40%, 50%) and assessed how these results correlated with the affected areas determined by field surveys (Figure 12).

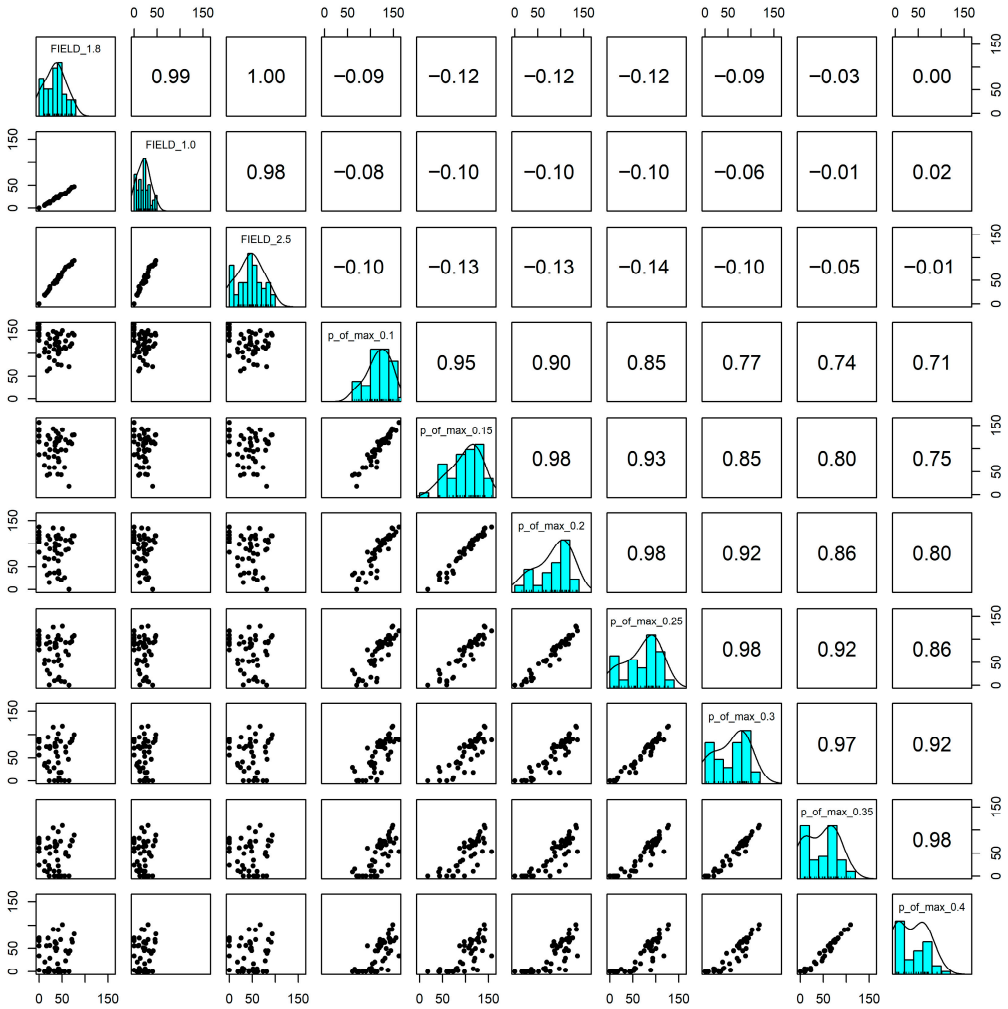

Figure 12. Scatterplot matrix showing the relationship between the estimates of affected areas derived from the GNSS-track approach using different threshold values and the affected areas determined by field surveys. Pearson correlation coefficients are shown above the diagonal.

Changing the threshold used to identify affected areas from GNSS tracks did not improve the correlation with the affected-area estimates obtained from field surveys, regardless of the temporal period of the GNSS data (2009–2024 or 2021–2024) (Figure 13). As the threshold increased, the estimated extent of affected areas decreased, mirroring the decrease observed when smaller buffer widths were used. Although Figure 13 shows that

higher thresholds produced estimates that were quantitatively more comparable to the field survey assessments, this did not translate into stronger correlations.

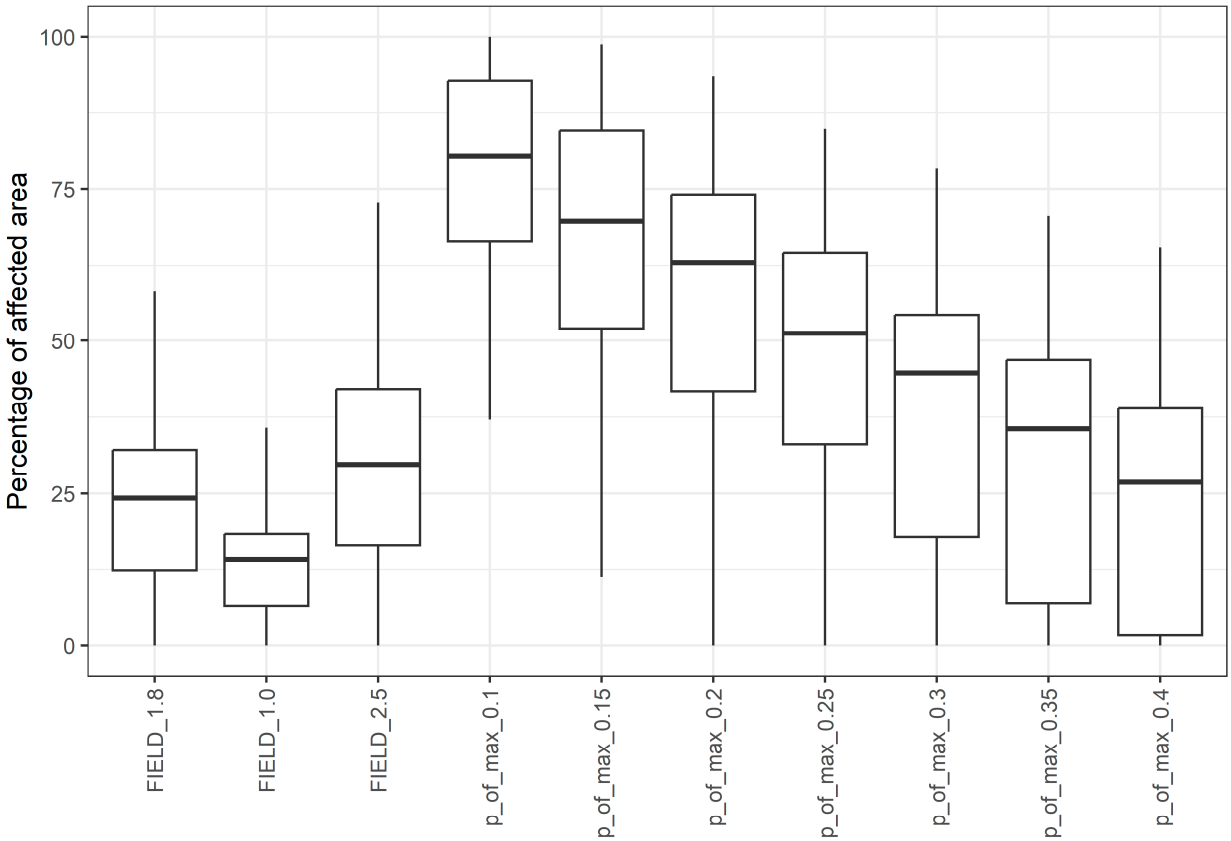

Figure 13. Distribution of the percentage of affected areas based on different threshold values applied in the GNSS-track approach for the 2009–2024 period.

By intersecting the affected areas determined using different approaches and buffer widths, we aimed to assess the degree of spatial overlap between the datasets—specifically, how well the results of the reference field surveys can be described and predicted using the displays and the GNSS tracks approaches.

Table 3 presents the descriptive statistics for the intersections. The intersection between the field surveys' affected areas and those derived from the GNSS tracks is larger when using a uniform width of 2.5 m—covering, on average, 19.2% of the test-plot area—whereas using a uniform width of 1 m results in a smaller intersection of 6.9%. The medians are slightly lower, indicating the presence of outliers and a skewed distribution, as also shown in Figure 14.

A similar pattern is observed for the intersection between the display-derived affected areas and those from the GNSS tracks, as well as for the overlap between display-derived areas and field survey areas: both are larger when a uniform width of 2.5 m is applied. The percentages simply reflect that using a larger width results in a bigger spatial intersection.

In addition to examining the degree of intersection between the datasets, we also investigated how well the relative extent of affected areas determined with field surveys can be predicted using the display-analysis approach, while accounting for other terrain characteristics (elevation, slope, substrate, and canopy cover—variables listed in Table S1, Supplementary Materials).

Table 3. Descriptive statistics for the relative estimates of affected areas determined from pairwise intersections of the approaches and applied widths. The minimum value is 0% in all cases. S_e denotes the standard error.

Approaches Intersection	Max (%)	Median (%)	Mean (%)	S_e (%)
RS_0.8_vs_FIELD_1.8	14.3%	3.9%	4.2%	0.6%
RS_0.8_vs_GNSS_2.5	17.9%	3.4%	4.7%	0.8%
RS_0.8_vs_GNNS_lines	15.3%	0.4%	2.7%	0.6%
RS_1.0_vs_FIELD_1.0	13.0%	2.8%	3.3%	0.5%
RS_1.0_vs_GNNS_1.0	20.6%	2.0%	4.5%	0.9%
RS_1.0_vs_GNNS_lines	18.8%	0.5%	3.4%	0.7%
RS_2.5_vs_FIELD_2.5	46.2%	13.4%	14.4%	1.9%
RS_2.5_vs_GNNS_2.5	51.1%	11.3%	14.1%	2.3%
RS_2.5_vs_GNNS_lines	39.8%	1.5%	7.9%	1.7%
FIELD_1.8_vs_GNNS_2.5	53.3%	11.4%	14.9%	2.1%
FIELD_1.8_vs_GNNS_lines	34.9%	2.7%	8.4%	1.5%
FIELD_1.0_vs_GNNS_1.0	28.8%	4.3%	6.9%	1.1%
FIELD_1.0_vs_GNNS_lines	23.1%	1.5%	5.0%	0.9%
FIELD_2.5_vs_GNNS_2.5	67.0%	14.4%	19.2%	2.6%
FIELD_2.5_vs_GNNS_lines	40.4%	4.1%	10.8%	1.9%

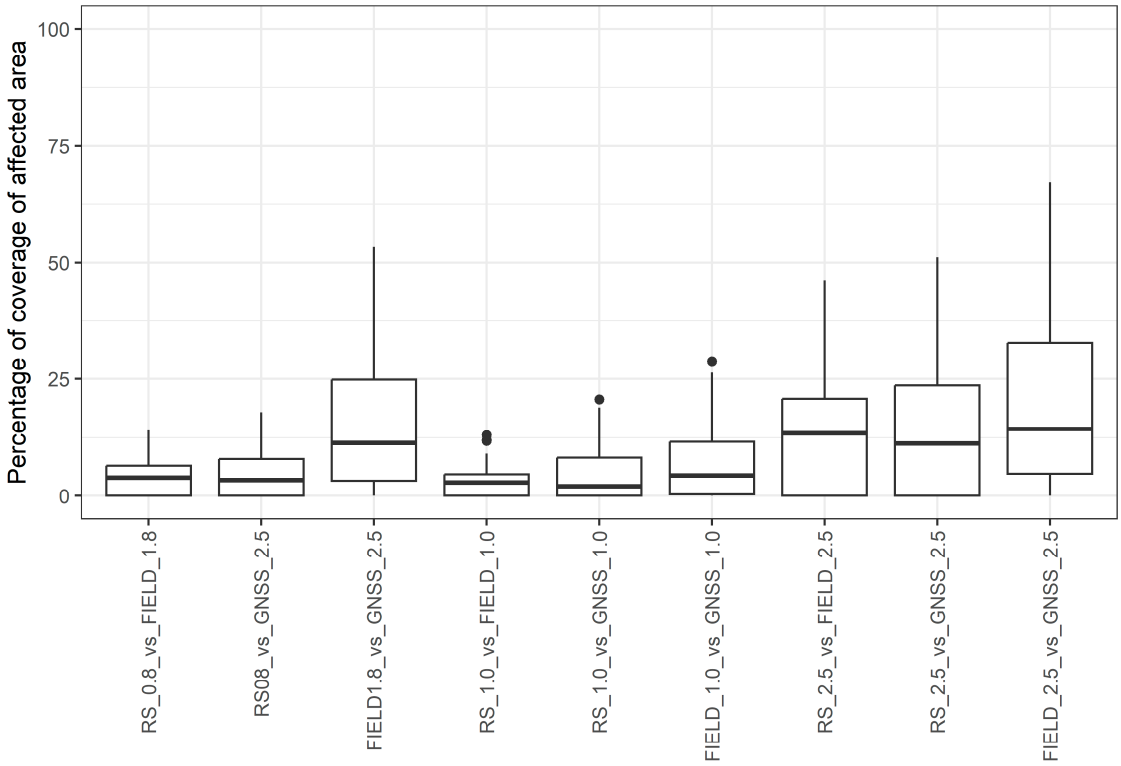

Figure 14. Distribution of the percentage of estimated affected areas determined from the intersections between the different approaches and applied widths.

Figure 11 shows that the strongest linear correlation exists between FIELD_2.5 and RS_2.5 (r = 0.73), and between FIELD_1.0 and RS_1.0 (r = 0.72). Using a linear regression model to predict FIELD_2.5 values based on RS_2.5 values gives a rather wide 95% confidence interval for the mean prediction of FIELD_2.5. To evaluate this, we calculated a

linear regression model (Figure 15). The results show that the display-analysis approach explains 52.7% of the variability in the field survey-determined affected areas when using the 2.5 m width. A similar proportion of explained variability (52.9%) was obtained with the 1 m width, although the estimated affected areas are substantially smaller on average, and the 95% confidence intervals for the mean prediction of FIELD_1.0 are narrower (Figure 15). We also found that adding additional terrain characteristics (elevation, slope, substrate, and canopy cover) as explanatory variables in the linear model did not explain a statistically significant additional part of the variability of FIELD_2.5 or FIELD_1.0, so these variables could not improve the prediction of the mean response.

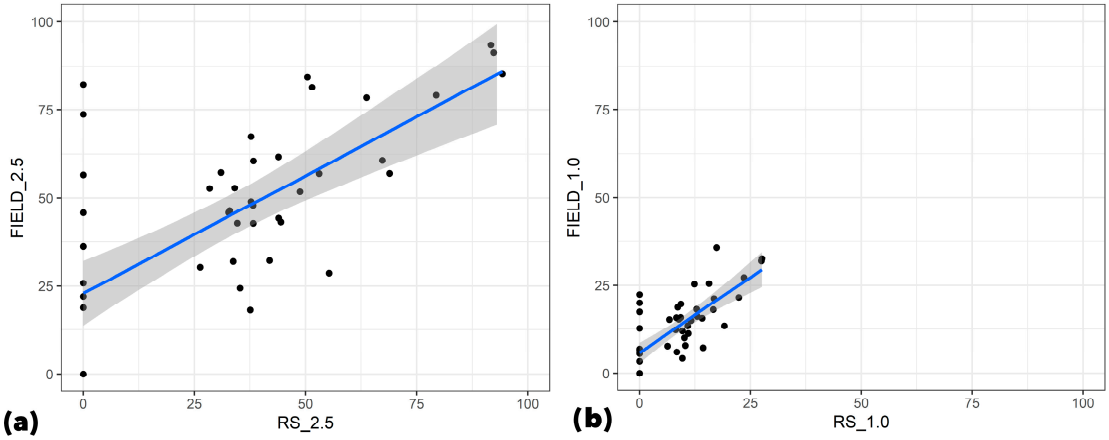

Figure 15. Predictions from the linear regression model with the corresponding 95% confidence intervals for the displays and field survey approaches, using buffer widths of 2.5 m (**a**) and 1 m (**b**).

In addition to the statistical comparison, Figure 16 provides a spatial perspective on the agreement between approaches.

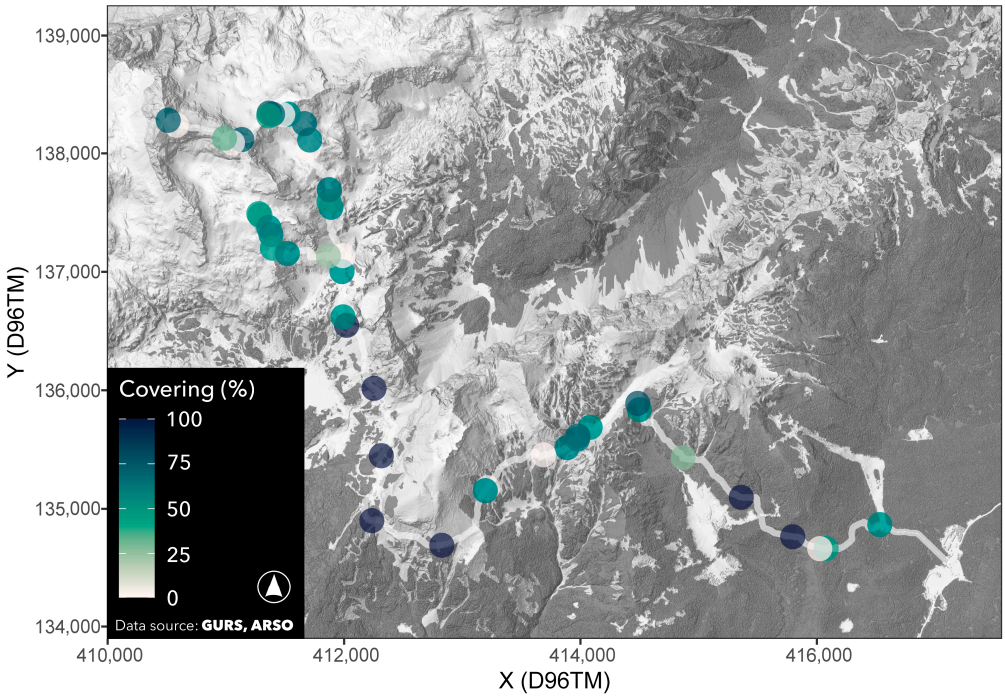

Figure 16. Spatial distribution of the relative intersection between display (RS_2.5) and field survey approaches (FIELD_2.5), shown against the field survey approach (FIELD_2.5).

Since there is no correlation between the estimates of affected areas determined through field surveys and those derived from GNSS tracks, we were likewise unable to develop a regression model that explains the field survey results using the GNSS track processing approach. We conclude that, given the approach applied, GNSS tracks do not provide enough information to predict affected areas with accuracy comparable to field surveys.

4. Discussion and Conclusions

In this study, we propose a new perspective for assessing areas affected by visitors moving outside the designated and maintained trails. The purpose of the research was to determine these affected areas, specifically to identify their locations and quantify their extent in square metres. We achieved this on 46 test plots along a selected mountain trail using three complementary approaches.

4.1. Commentary on the Approaches

We obtained reference data through field surveys and used them to compare and evaluate the other two approaches. Despite certain limitations (positional accuracy of the device, satellite availability, current weather conditions, etc.), field surveys proved to be the most reliable, unambiguous, and direct approach for determining the actual affected areas, as was already tested in other mountainous areas [88]. By consistently following the selected mountain trail, we were able—through systematic visual examination of the test plots—to reliably distinguish affected areas from the trail surface, delineate their course and map their extent. Even on sections where following the mountain trail was more challenging, considering the broader spatial context (the trail's route and surrounding features) enabled us to distinguish between the trail surface itself and the affected areas. Following the trail within this broader context, at a smaller scale, also proved highly effective when identifying affected areas in the ALS visualisations.

The concern that young, seasonal undergrowth might obscure affected areas and lead to their omission during field surveys proved unnecessary. In fact, the results showed the opposite—field surveys enabled us to map affected areas even on test plots where they could not be determined using ALS visualisations.

We were unable to distinguish affected areas clearly on test plots that were almost entirely eroded, which made it impossible to map their centrelines with the surveying device. Defining test plots based on the device's measurement functions was therefore not an ideal solution; however, this approach was chosen intentionally, as the field survey was conducted in extremely difficult and exposed terrain, in some cases requiring the use of protective self-belay equipment. Because fieldwork is inherently time-consuming and costly [32,89], it would represent a considerable challenge for park managers, especially in such a demanding environment. Therefore, we tested whether adequate results could be obtained through the analysis of displays and GNSS tracks, which has also already been the case in other recreation areas [90]. Moreover, sampling other local physical variables could help to assess the effects of hiking on erosion [91].

When analysing the combined visualisations of airborne laser scanning (ALS) data and the aerial orthophoto, we found that many affected areas could be identified from the aerial orthophoto alone. In sections where the trail ran beneath tree canopy, ALS data proved highly useful for detecting affected areas. However, the combined visualisations were less reliable on fully rocky surfaces—those lacking soil, debris, sand, and scree—and in sections with pronounced surface erosion.

These limitations can also be attributed to the challenges related to performing field work in an area with rugged terrain with potentially unsafe conditions and common sudden

changes to weather conditions, which is difficult to access and has a large altitudinal range, that also limits the amount of potential return visits. Between 1347 m a.s.l and approximately 1700 m a.s.l., test plots were located in forested environments with well-developed humus layers, which enable affected areas to be clearly recognisable by displays.

With elevation, determination of affected areas gradually decreased: up to around 1900 m a.s.l., where sparse low vegetation provided some indication of off-trail surface disturbance, whereas above this elevation the terrain was almost entirely open and rocky, with minimal vegetation cover (see Table S1, Supplementary Materials). Under such geomorphological conditions, affected areas leave weaker or no structural traces, which reduces their detectability by using displays analysis approach.

In the third approach—the analysis of GNSS tracks—we sought to make the data more comparable to the other two approaches by standardising the buffer widths (1 m and 2.5 m) and applying a threshold. This allowed us to identify areas affected by long-term, spontaneous movement outside the designated mountain trail, despite the large number of GNSS tracks and their varying positional accuracy.

A major limitation of our approach is, that the process of manually downloading and processing GNSS tracks, constrained by download rules, security protocols, and the technical limitations of each application's user interface, proved time consuming and technically demanding. Nevertheless, these data are also the most variable, reflecting differences in devices used, application performance, rapid changes in user accounts, functionalities, levels of accessibility, and continuous updates, as applications aim to remain attractive and engaging for users [92]. This makes volunteered information on recreation a useful piece of information for park managers and other researchers [93].

4.2. Commentary on the Results

We determined the location of affected areas on the test plots by all three approaches. Wherever affected areas were detected through the display's analysis or GNSS tracks, they were also confirmed by field surveys. These findings support previous studies that have demonstrated the correspondence between GNSS tracks and field surveys and highlighted their usefulness for identifying areas with high use intensity and a greater density of affected surfaces [27,28,32,94].

The results show that field surveys and the display's analysis are correlated, and that the latter approach can explain 52.7% of the variability in the former when using a width of 2.5 m, and 52.9% when using a width of 1 m.

We found that the number of GNSS tracks from a single season (471 tracks from 2024) is fully representative of longer periods and can adequately reflect affected areas resulting from long-term off-trail movement. However, regardless of the temporal range or the width applied, the results derived from GNSS tracks show no correlation with the other two approaches. Consequently, GNSS tracks did not allow us to develop a regression model capable of describing or predicting the affected-area estimates obtained through field surveys. Despite the usefulness and widespread availability of GNSS data on recreation, our results indicate that as standalone data, GNSS tracks alone are insufficient to identify potential erosion recreational areas.

In analysing the intersections of estimated affected areas across the different approaches, we found, as expected, that the intersections were largest when using the uniform width of 2.5 m. On average, the intersection between field surveys and GNSS track processing accounted for 19.2% of the test plot area, the intersection between field surveys and displays for 14.1%, and the intersection between displays and GNSS track processing for 14.4% of the test plot area. These intersection results suggest that such comparative analyses remain relevant for future research, particularly as technological advances will

provide data with substantially higher spatial resolution and positional accuracy, thereby enabling substantially better spatial intersection.

These limitations are particularly applicable to GNSS tracks, where the key constraints are their variability and positional accuracy [32,81]. Despite this, GNSS tracks provide highly valuable and, above all, up-to-date information on the spontaneous and dynamic movement of visitors within an area, movement that cannot be fully anticipated or its consequences reliably predicted. Such information is particularly important for site managers, as it enables them to adapt planning and management practices accordingly [32]. GNSS tracks represent only a small fraction of the actual movement of users [28], implying that the extent of affected areas is likely even greater.

The proposed method demonstrates that each of the three approaches can be used to determine the location of affected areas and quantify their extent (in m^2) beyond the designated mountain trail surface. The method also highlights its dependence on the positional accuracy of the available input data and the technical complexity of their processing. Although the two approaches based on displays and GNSS tracks cannot yet reliably explain or predict the field survey estimates of affected areas, the results show that the three approaches complement each other effectively and are best applied in combination. This is further supported by the successful correction of the mountain trail alignment achieved through their integrated use.

Combining the three approaches also proves valuable for determining the affected areas. Where displays do not reveal affected surfaces, but GNSS tracks suggest their presence, targeted field verification is warranted. Conversely, when GNSS tracks indicate multiple potential locations, displays can help determine the precise location and spatial extent of these affected areas, enabling the field survey to be directed more efficiently. An important advantage of combining the approaches is that, whereas field surveys and displays detect affected areas only once they are already clearly visible in the landscape, GNSS tracks allow us to identify affected areas before they become pronounced as a result of repeated use.

In addition to its application in high-mountain areas, the proposed methodology can be applied in other recreational areas and along different types of trails, including those in urban settings. Especially in the latter, it may support the planning and management of open green spaces and recreation-related infrastructure.

Furthermore, the introduction of a measurable indicator provides an important added value, as it enables precise identification and quantification of changes and impacts occurring within a defined area over a specific period. It can support protected-area managers and conservation professionals in prioritising and directing/targeting their interventions in the most problematic areas.

Our study demonstrates that the affected area, expressed as the surface area (m^2) outside the designated trail, serves as a meaningful indicator of the actual extent of environmental impacts. With continued technological advances and improved data accuracy, this indicator will be measurable with increasing precision. When combined with information on visitor numbers and overlayed with spatial vulnerability maps, it holds substantial potential for assessing landscape and ecosystem degradation, evaluating impacts, and defining thresholds for acceptable (sustainable) visitor use. This could help prevent the emergence of negative trends associated with existing infrastructure [5] by identifying pressures before they become significant and irreversible.

Supplementary Materials: The following supporting information can be downloaded at: https://www.mdpi.com/article/10.3390/land15010200/s1, Table S1: List of test plots with descriptions of their characteristics.

Author Contributions: Conceptualization, A.B., M.G., Ž.M. and Ž.K.; methodology, A.B., D.K., Ž.M. and Ž.K.; software, A.B., D.K. and Ž.K.; validation, A.B., D.K. and Ž.K.; formal analysis, A.B., D.K.; investigation, A.B.; resources, A.B.; data curation, A.B.; writing—original draft preparation, A.B.; writing—review and editing, A.B., D.K., M.G., Ž.M. and Ž.K.; visualisation, A.B.; supervision, M.G., Ž.K.; project administration, A.B., M.G. and Ž.K.; funding acquisition, M.G. and Ž.K. All authors have read and agreed to the published version of the manuscript.

Funding: This research was funded by University of Ljubljana, project P40009: Landscape as Living Environment and by the Slovenian Research and Innovation Agency core funding Earth observation and geoinformatics (P2-0406) and the research project Geospatial information technologies for resilient and sustainable society (GC-0006).

Data Availability Statement: The data is available from the authors upon reasonable request.

Acknowledgments: We would like to thank Drew Flater from Esri for the Average Line tool development.

Conflicts of Interest: The authors declare no conflicts of interest. The funders had no role in the design of the study; in the collection, analyses, or interpretation of data; in the writing of the manuscript; or in the decision to publish the results.

References

1. Salerno, F.; Viviano, G.; Manfredi, E.C.; Caroli, P.; Thakuri, S.; Tartari, G. Multiple Carrying Capacities from a Manage-ment-Oriented Perspective to Operationalize Sustainable Tourism in Protected Areas. *J. Environ. Manag.* **2013**, *128*, 116–125. [CrossRef] [PubMed]
2. Načrt Upravljanja Triglavskega Narodnega Parka 2016–2025. 2016. Available online: https://www.tnp.si/media/1458/jz_tnp_nacrt_upravljanja_tnp_2016_2025.pdf (accessed on 13 March 2021).
3. Kuba, K.; Monz, C.; Bårdsen, B.-J.; Hausner, V.H. Role of Site Management in Influencing Visitor Use along Trails in Multiple Alpine Protected Areas in Norway. *J. Outdoor Recreat. Tour.* **2018**, *22*, 1–8. [CrossRef]
4. Barros, A.; Aschero, V.; Mazzolari, A.; Cavieres, L.A.; Pickering, C.M. Going off Trails: How Dispersed Visitor Use Affects Alpine Vegetation. *J. Environ. Manag.* **2020**, *267*, 110546. [CrossRef]
5. Rawat, M.; Jägerbrand, A.K.; Molau, U.; Bai, Y.; Alatalo, J.M. Visitors off the Trail: Impacts on the Dominant Plant, Bryophyte and Lichen Species in Alpine Heath Vegetation in Sub-Arctic Sweden. *Environ. Chall.* **2021**, *3*, 100050. [CrossRef]
6. Jodłowski, M.; Rechciński, M. Model of High-Mountain Hiking Trails (via Ferrata Type) in Tatra National Park—A Comparison between Poland and Slovakia in the Context of the Alps. Available online: https://mmv.boku.ac.at/refbase/files/mmv6_146_147.pdf (accessed on 25 September 2024).
7. Lawson, S.R.; Manning, R.E.; Valliere, W.A.; Wang, B. Proactive Monitoring and Adaptive Management of Social Carrying Capacity in Arches National Park: An Application of Computer Simulation Modeling. *J. Environ. Manag.* **2003**, *68*, 305–313. [CrossRef]
8. Luque-Gil, A.M.; Gómez-Moreno, M.L.; Peláez-Fernández, M.A. Starting to Enjoy Nature in Mediterranean Mountains: Crowding Perception and Satisfaction. *Tour. Manag. Perspect.* **2018**, *25*, 93–103. [CrossRef]
9. Yin, J.; Cheng, Y.; Bi, Y.; Ni, Y. Tourists Perceived Crowding and Destination Attractiveness: The Moderating Effects of Perceived Risk and Experience Quality. *J. Destin. Mark. Manag.* **2020**, *18*, 100489. [CrossRef]
10. Sæþórsdóttir, A.D.; Hall, C.M. Visitor Satisfaction in Wilderness in Times of Overtourism: A Longitudinal Study. *J. Sustain. Tour.* **2020**, *29*, 123–141. [CrossRef]
11. Peng, L.; Su, J.; Zhang, N.; Cui, Y. Social Crowding Increases Tourists' Preference for Natural Products: The Effect of Ontological Security Threat and Social Connectedness. *J. Sustain. Tour.* **2025**, *33*, 2577–2596. [CrossRef]
12. Garcia-Massó, X.; Muhar, A.; Brandenburg, C.; Toca-Herrera, J.-L. Evaluating the Structure and Use of Hiking Trails in Recreational Areas Using a Mixed GPS Tracking and Graph Theory Approach. *Appl. Geogr.* **2014**, *55*, 184–192. [CrossRef]
13. Tomczyk, A.M.; Ewertowski, M.W.; White, P.C.L.; Kasprzak, L. A New Framework for Prioritising Decisions on Recreational Trail Management. *Landsc. Urban Plan.* **2017**, *167*, 1–13. [CrossRef]
14. Wimpey, J.F.; Marion, J.L. The Influence of Use, Environmental and Managerial Factors on the Width of Recreational Trails. *J. Environ. Manag.* **2010**, *91*, 2028–2037. [CrossRef] [PubMed]
15. Meadema, F.; Marion, J.L.; Arredondo, J.; Wimpey, J. The Influence of Layout on Appalachian Trail Soil Loss, Widening, and Muddiness: Implications for Sustainable Trail Design and Management. *J. Environ. Manag.* **2020**, *257*, 109986. [CrossRef]
16. Wimpey, J.; Marion, J.L. A Spatial Exploration of Informal Trail Networks within Great Falls Park, VA. *J. Environ. Manag.* **2011**, *92*, 1012–1022. [CrossRef]

17. Marion, J.L.; Leung, Y.-F. Trail Resource Impacts and an Examination of Alternative Assessment Techniques. *J. Park Recreat. Adm.* **2001**, *19*, 17–37.
18. Miller, A.B.; Kays, R.; Leung, Y.-F. Wildlife Response to Recreational Trail Building: An Experimental Method and Appalachian Case Study. *J. Nat. Conserv.* **2020**, *56*, 125815. [CrossRef]
19. Tverijonaite, E.; Sæþórsdóttir, A.D.; Ólafsdóttir, R.; Hall, C.M. Wilderness: A Resource or a Sanctuary? Views of Tourism Service Providers. *Scand. J. Hosp. Tour.* **2023**, *23*, 195–225. [CrossRef]
20. Marion, J.L. Trail Sustainability: A State-of-Knowledge Review of Trail Impacts, Influential Factors, Sustainability Ratings, and Planning and Management Guidance. *J. Environ. Manag.* **2023**, *340*, 117868. [CrossRef] [PubMed]
21. Liedtke, R.; Barros, A.; Essl, F.; Lembrechts, J.J.; Wedegärtner, R.E.M.; Pauchard, A.; Dullinger, S. Hiking Trails as Conduits for the Spread of Non-Native Species in Mountain Areas. *Biol. Invasions* **2020**, *22*, 1121–1134. [CrossRef]
22. D'Antonio, A.; Monz, C. The Influence of Visitor Use Levels on Visitor Spatial Behavior in Off-Trail Areas of Dispersed Recreation Use. *J. Environ. Manag.* **2016**, *170*, 79–87. [CrossRef] [PubMed]
23. Monz, C.A.; Cole, D.N.; Leung, Y.-F.; Marion, J.L. Sustaining Visitor Use in Protected Areas: Future Opportunities in Recreation Ecology Research Based on the USA Experience. *Environ. Manag.* **2010**, *45*, 551–562. [CrossRef]
24. Stamberger, L.; van Riper, C.J.; Keller, R.; Brownlee, M.; Rose, J. A GPS Tracking Study of Recreationists in an Alaskan Protected Area. *Appl. Geogr.* **2018**, *93*, 92–102. [CrossRef]
25. Evju, M.; Hagen, D.; Jokerud, M.; Olsen, S.L.; Selvaag, S.K.; Vistad, O.I. Effects of Mountain Biking versus Hiking on Trails under Different Environmental Conditions. *J. Environ. Manag.* **2021**, *278*, 111554. [CrossRef]
26. Fisher, D.M.; Wood, S.A.; White, E.M.; Blahna, D.J.; Lange, S.; Weinberg, A.; Tomco, M.; Lia, E. Recreational Use in Dispersed Public Lands Measured Using Social Media Data and On-Site Counts. *J. Environ. Manag.* **2018**, *222*, 465–474. [CrossRef]
27. Taczanowska, K.; Muhar, A.; Brandenburg, C. Potential and Limitations of GPS Tracking for Monitoring Spatial and Temporal Aspects of Visitor Behaviour in Recreational Areas. 2008. Available online: https://mmv.boku.ac.at/refbase/files/taczanowska_karolin-2008-potential_and_limita.pdf (accessed on 23 July 2021).
28. Norman, P.; Pickering, C.M. Using Volunteered Geographic Information to Assess Park Visitation: Comparing Three on-Line Platforms. *Appl. Geogr.* **2017**, *89*, 163–172. [CrossRef]
29. Meijles, E.W.; de Bakker, M.; Groote, P.D.; Barske, R. Analysing Hiker Movement Patterns Using GPS Data: Implications for Park Management. *Comput. Environ. Urban Syst.* **2014**, *47*, 44–57. [CrossRef]
30. Eagleston, H.; Marion, J.L. Application of Airborne LiDAR and GIS in Modeling Trail Erosion along the Appalachian Trail in New Hampshire, USA. *Landsc. Urban Plan.* **2020**, *198*, 103765. [CrossRef]
31. Salesa, D.; Cerdà, A. Soil Erosion on Mountain Trails as a Consequence of Recreational Activities. A Comprehensive Review of the Scientific Literature. *J. Environ. Manag.* **2020**, *271*, 110990. [CrossRef]
32. Korpilo, S.; Virtanen, T.; Lehvävirta, S. Smartphone GPS Tracking—Inexpensive and Efficient Data Collection on Recreational Movement. *Landsc. Urban Plan.* **2017**, *157*, 608–617. [CrossRef]
33. Wolf, I.D.; Wohlfart, T.; Brown, G.; Bartolomé Lasa, A. The Use of Public Participation GIS (PPGIS) for Park Visitor Management: A Case Study of Mountain Biking. *Tour. Manag.* **2015**, *51*, 112–130. [CrossRef]
34. Lotrič, U.; Mikoš, M.; Golja, A. Water-Related Sports Activities in the Triglav National Park, Slovenia—Part 1 Hydrological Basis. *Acta Hydrotech.* **2015**, *28*, 15.
35. Zdešar, A. Carrying Capacity in Triglav National Park, Animal Habitats and Visitor Safety. *Pers. Commun.* **2021**.
36. Kralj, T. Environmental Carrying Capacity through Management Aspects of the Triglav National Park. *Pers. Commun.* **2021**.
37. Alpine Association of Slovenia; LUZ d.d. maPZS. Available online: https://mapzs.pzs.si/about?lang=en (accessed on 15 April 2021).
38. Flater, D. Understanding Geodesic Buffering. Available online: https://docslib.org/doc/10502242/understanding-geodesic-buffering-correctly-use-the-buffer-tool-in-arcgis-by-drew-flater-esri-geoprocessing-development-team (accessed on 7 March 2025).
39. ESRI—Environmental Systems Research Institute. Buffer (Analysis). ArcGIS Pro 3.3.5. Available online: https://tech-support.esrij.com/arcgis/article/web/knowledge5892.html (accessed on 7 March 2025).
40. Hazzard, C. Garmin GPSMAP 66sr Review and Test. *HikingGuy* 2021. Available online: https://hikingguy.com/hiking-gear/garmin-gpsmap-66sr-review-test/ (accessed on 12 February 2025).
41. Garmin. Garmin Connect. Available online: https://connect.garmin.com/ (accessed on 15 April 2024).
42. Suunto. Suunto App for Getting the Most out Your Suunto Watch. Available online: https://www.suunto.com/suunto-app/suunto-app-2022/ (accessed on 3 December 2025).
43. AllTrails. AllTrails: Trail Guides and Maps for Hiking, Camping, and Running. Available online: https://www.alltrails.com/ (accessed on 15 April 2024).
44. FATMAP. The FATMAP Map Is Coming to Strava. Available online: https://www.strava.com/legacy-embeds (accessed on 3 December 2025).
45. Gaia GPS. Gaia GPS: Hiking Trail Maps, Ski Touring, 4x4 Offroad App. Available online: https://www.gaiagps.com/ (accessed on 15 April 2024).

46. Komoot. Komoot | Find, Plan and Share Your Adventures. Available online: https://www.komoot.com (accessed on 3 December 2025).
47. Relive. Relive | Run, Ride, Hike & More. Available online: https://www.relive.com (accessed on 3 December 2025).
48. Sports Tracker. Sports Tracker. Available online: https://www.sports-tracker.com/ (accessed on 3 December 2025).
49. Strava. Strava | Running, Cycling & Hiking App—Train, Track & Share. Available online: https://www.strava.com/ (accessed on 3 December 2025).
50. Wikiloc. Wikiloc | Trails of the World. Available online: https://www.wikiloc.com (accessed on 15 April 2024).
51. Public Infrastructure Cadastre. 2025. Available online: https://ipi.eprostor.gov.si/jgp/data (accessed on 12 February 2025).
52. Flater, D. Average Lines. ArcGIS Pro 3.2.2. 2024. Available online: https://support.esri.com/ja-jp/patches-updates/2024/arcgis-pro-3-2-patch-2-3-2-2-announcement (accessed on 13 February 2024).
53. GURS. The Surveying and Mapping Authority of the Republic of Slovenia. Ministry of Natural Resources and Spatial Planning. Ljubljana. Public Geodetic Data. Available online: https://ipi.eprostor.gov.si/jgp/data (accessed on 27 October 2023).
54. ARSO; Slovenian Environment Agency; Ljubljana. Atlas Okolja. Lidar GIS Viewer. 2023. Available online: https://services8.arcgis.com/ZYlQy38aWlfDG1Qh/ArcGIS/rest/services/Lidar_2023/FeatureServer (accessed on 27 October 2023).
55. Pegan Žvokelj, B.; Bric, V.; Triglav Čekada, M. Laser Scanning in Slovenia. *Geod. Vestn.* **2014**, *58*, 349–351.
56. Kokalj, Ž. Laser Scanning of Slovenia—Implementation and Results of the Highland Survey. *Pers. Commun.* **2024**.
57. Childs, C. Interpolating Surfaces in ArcGIS Spatial Analyst. *ArcUser* **2004**, *3235*, 32–35.
58. GIS Resources. Types of Interpolation—Advantages and Disadvantages. *GIS Resources*. 2023. Available online: https://gisresources.com/types-interpolation-methods_3/ (accessed on 11 November 2023).
59. Stereńczak, K.; Ciesielski, M.; Balazy, R.; Zawiła-Niedźwiecki, T. Comparison of Various Algorithms for DTM Interpolation from LIDAR Data in Dense Mountain Forests. *Eur. J. Remote Sens.* **2016**, *49*, 599–621. [CrossRef]
60. Hobič, J. Od Oblaka Do Pokrajine. Razširjena Navodila za »obdelavo« in Vizualizacijo LiDAR Podatkov. Available online: https://arheologija.neocities.org/lidar_navodila (accessed on 4 November 2023).
61. Kokalj, Ž.; Zakršek, K.; Oštir, K.; Somrak, M. Relief Visualization Toolbox. Python. V. 2.1.0. Available online: https://rvt-py.readthedocs.io/en/latest/ (accessed on 11 November 2025).
62. Kokalj, Ž.; Maroh, Ž.; Oštir, K.; Doerffel, G.; Čož, N. ArcGIS Pro Relief Visualization Toolbox Raster Functions. Python. V. 2.2.1. 2025. Available online: https://github.com/EarthObservation/rvt-arcgis-pro (accessed on 11 November 2025).
63. Kokalj, Ž.; Somrak, M. Why Not a Single Image? Combining Visualizations to Facilitate Fieldwork and On-Screen Mapping. *Remote Sens.* **2019**, *11*, 747. [CrossRef]
64. Zakšek, K.; Oštir, K.; Kokalj, Ž. Sky-View Factor as a Relief Visualization Technique. *Remote Sens.* **2011**, *3*, 398–415. [CrossRef]
65. Barker, J. 9 Best Apps for Hiking and Backpacking. *Hiking Daily*. 2021. Available online: https://hikingdaily.com/category/best-hikes/ (accessed on 22 January 2021).
66. Tedesco, L. These Are the Best Hiking Apps You Can Have for the Trails in 2021. Available online: https://www.thetravel.com/archive/2/ (accessed on 26 March 2021).
67. Watson, P. 15 Best Hiking Apps to Download in 2025. Atlas and Boots. 2025. Available online: https://www.atlasandboots.com/travel-blog/best-hiking-apps/ (accessed on 26 March 2025).
68. Weingus, L. The 14 Best Hiking Apps So You Can Hit the Trails All Spring Long (Without Getting Lost!). Available online: https://parade.com/1186154/leighweingus/best-hiking-apps/ (accessed on 31 May 2021).
69. Hub, G. The Best Hiking Apps 2022. Glamping Hub Blog. 2022. Available online: https://glampinghub.com/blog/best-hiking-apps/ (accessed on 10 November 2022).
70. 17 Best Hiking Apps for 2022. Take a Hike! 2022. Available online: https://www.voyageurtripper.com/best-hiking-apps/ (accessed on 5 May 2022).
71. Dean, D. 10 of the Best Hiking Apps to Download Before You Hit the Trail. Too Many Adapters. 2023. Available online: https://toomanyadapters.com/hiking-apps/ (accessed on 10 May 2023).
72. Best Hiking Apps of 2024—Tested and Reviewed. Nail the Trail. 2024. Available online: https://nailthetrail.com/best-hiking-apps-test-review/ (accessed on 13 March 2024).
73. Hill, S. Best Hiking Apps Guide for iPhone and Android. Explore the Map. 2025. Available online: https://explorethemap.com/hiking-apps/ (accessed on 22 March 2025).
74. Jones, J. 17 Best Hiking Apps You Should Download Today. Well Planned Journey. 2025. Available online: https://www.wellplannedjourney.com/best-hiking-apps/ (accessed on 14 April 2025).
75. Licavoli, K. 10 Best Hiking Apps for 2025. Available online: https://www.greenbelly.co/pages/best-hiking-apps (accessed on 7 February 2025).
76. Hiking Project Hiking Project | Hiking Trail Maps. Available online: https://hikingproject.com (accessed on 3 December 2025).

77. MapMyFitness. MapMyFitness—Reach Your Best. Workout Smarter. Available online: https://www.mapmyfitness.com/ (accessed on 3 December 2025).
78. Outdooractive. Outdooractive. Available online: https://www.outdooractive.com/en/ (accessed on 15 April 2024).
79. Suunto Stay Connected—Transfer from Suunto Movescount to Suunto App. Available online: https://www.suunto.com/Content-pages/digital-service-transition/ (accessed on 3 December 2025).
80. Gpx.Studio—The Online GPX File Editor. Available online: https://gpx.studio/ (accessed on 16 November 2024).
81. Hess, B.; Farahani, A.Z.; Tschirschnitz, F.; Von Reischach, F. Evaluation of Fine-Granular GPS Tracking on Smartphones. In *Proceedings of the First ACM SIGSPATIAL International Workshop on Mobile Geographic Information Systems*; ACM: Redondo Beach, CA, USA, 2012; pp. 33–40.
82. Tomaštík, J.; Tomaštík, J.; Saloň, Š.; Piroh, R. Horizontal Accuracy and Applicability of Smartphone GNSS Positioning in Forests. *Forestry* **2016**, *90*, 187–198. [CrossRef]
83. Paziewski, J. Recent Advances and Perspectives for Positioning and Applications with Smartphone GNSS Observations. *Meas. Sci. Technol.* **2020**, *31*, 091001. [CrossRef]
84. Huang, J.; Guo, Y.; Li, X.; Zhang, N.; Jiang, J.; Wang, G. Evaluation of Positioning Accuracy of Smartphones under Different Canopy Openness. *Forests* **2022**, *13*, 1591. [CrossRef]
85. Schinagl, H. Mobile Phones and Mobile GIS. Available online: https://www.terralabgis.com/blog/mobile-phones-and-mobile-gis (accessed on 27 January 2025).
86. Mikoś, M.; Kazmierski, K.; Wachulec, N.; Sośnica, K. Accuracy of Satellite Positioning Using GNSS Receivers in Sports Watches. *Measurement* **2024**, *229*, 114426. [CrossRef]
87. Jordan, B.; Selinger, B.; Rovan, J.; Tomše, T. *Priročnik Za Markaciste: Učbenik, Gradivo za Usposabljanje Markacistov PZS*; Planinska zveza Slovenije: Ljubljana, Slovenia, 2009.
88. Barros, A.; Marina Pickering, C. How Networks of Informal Trails Cause Landscape Level Damage to Vegetation. *Environ. Manag.* **2017**, *60*, 57–68. [CrossRef]
89. Walden-Schreiner, C.; Leung, Y.-F. Spatially Characterizing Visitor Use and Its Association with Informal Trails in Yosemite Valley Meadows. *Environ. Manag.* **2013**, *52*, 163–178. [CrossRef] [PubMed]
90. Campelo, M.B.; Nogueira Mendes, R.M. Comparing Webshare Services to Assess Mountain Bike Use in Protected Areas. *J. Outdoor Recreat. Tour.* **2016**, *15*, 82–88. [CrossRef]
91. Ólafsdóttir, R.; Runnström, M.C. Assessing Hiking Trails Condition in Two Popular Tourist Destinations in the Icelandic Highlands. *J. Outdoor Recreat. Tour.* **2013**, *3–4*, 57–67. [CrossRef]
92. Teles da Mota, V.; Pickering, C. Using Social Media to Assess Nature-Based Tourism: Current Research and Future Trends. *J. Outdoor Recreat. Tour.* **2020**, *30*, 100295. [CrossRef]
93. Norman, P.; Pickering, C.M. Factors Influencing Park Popularity for Mountain Bikers, Walkers and Runners as Indicated by Social Media Route Data. *J. Environ. Manag.* **2019**, *249*, 109413. [CrossRef]
94. Wolf, I.D.; Hagenloh, G.; Croft, D.B. Visitor Monitoring along Roads and Hiking Trails: How to Determine Usage Levels in Tourist Sites. *Tour. Manag.* **2012**, *33*, 16–28. [CrossRef]